

AN ABSTRACT OF THE THESIS OF

Dakota Jacobs for the degree of Master of Science in Toxicology presented on September 16, 2016.

Title: Effect of PFAS Exposure on Reproduction; A Comparative Investigation Between Kisspeptin-secreting AVPV and Arcuate Nuclei

Abstract approved: _____

Patrick E. Chappell

Ovulation requires preovulatory surges of gonadotropin-releasing hormone (GnRH) from preoptic hypothalamic neurons, initiated by elevated ovarian estradiol (E_2). Rising estradiol activates a subset of sexually dimorphic kisspeptin (Kiss-1) neurons in the female, located in the anteroventral periventricular nuclei (AVPV). Conversely, estradiol negative feedback on GnRH secretion is mediated by a neuroanatomically separate population of Kiss-1 neurons in the arcuate nuclei. Kisspeptin stimulates GnRH expression and secretion *in vivo*, and the development of this system is critical for the initiation of puberty. To elucidate how phenotypically similar Kiss-1 neuronal populations react differentially to estradiol exposure, we have generated two immortalized Kiss-1 cell lines from *kiss1*-GFP post-pubertal female mice. These cell models recapitulate *in vivo* differential responsiveness to estradiol, with KTaV-3 (AVPV-derived) demonstrating ~6-fold increases in *kiss1* expression under higher estradiol doses (5pM – 50pM E_2), while *kiss1* expression in KTaR-1 cells is suppressed up to 80% under lower E_2 concentrations (2pM – 10pM). We probed temporal patterns of *kiss1* and core clock gene expression in these lines in response to estradiol, and found distinct antiphasic patterns of *bmal1* and *per2* in KTaV-3 cells irrespective of estradiol exposure. Treatment of KTaV-3 cells with 25pM E_2 , however, elicited distinct patterns of *kiss1* expression over time in contrast to vehicle, suggesting differential coupling of intracellular

oscillators to *kiss1* transcriptional activity in the presence of estradiol. Further, we have found that expression alterations between nuclear receptor ER α and ER β genes, *esr1* and *esr2*, respectively, fluctuate divergently between these lines. We have implicated that the peaks of *kiss1* expression demonstrated by the KTaV-3 lines may be mediated by both classical and non-classical estrogen signaling. In addition, we provide evidence that the negative regulation of *kiss1* expression in KTaR-1 cells may be a function of mutual antagonism due to overabundance of contemporaneously expressed *esr1* and *esr2* genes that is not observed in KTaV-3 lines. Lastly, we explored the impact of an endocrine disrupting class of perfluorinated alkyl substances (PFASs) on these neurons, with preliminary results illustrating *kiss1*, *esr1*, and *esr2* transcriptional activation and/or repression at relevant doses of perfluorooctanoic acid (PFOA), perfluorooctanesulfonic acid (PFOS), and perfluorohexanoic acid (PFHxA) in the two lines. At extremely low doses of PFOA, typical estrogenic demonstrations of *kiss1* expression are presented by KTaV-3 and KTaR-1 neurons. However at the same dose of PFOS the expression modulation of *kiss1* gated by estrogen signaling in this hypothalamic populations is flipped. This implicates that a sufficient exposure to these ubiquitous chemicals can have a potent effect on neuronal expression profiles for estrogen sensitive genes that is a complex function of dose, particular PFAS, and tissue type. Ongoing delineation of responsiveness to estradiol in these lines could reveal novel molecular mechanisms underlying differential expression patterns demonstrated *in vivo* between these neuronal populations. Furthermore, investigating the impact of select PFASs on secretory dynamics of kisspeptin and on the activity ER α and ER β between these two cell lines could elucidate the consequence of estrogen mimicry during sex-steroid sensitive developmental phases.

©Copyright by Dakota Jacobs
September 16, 2016
All Rights Reserved

Effect of PFAS Exposure on Reproduction: a Comparative Investigation between Kisspeptin-secreting AVPV and Arcuate Nuclei

by
Dakota Jacobs

A THESIS

submitted to

Oregon State University

in partial fulfillment of
the requirements for the
degree of

Master of Science

Presented September 16, 2016
Commencement June 2017

Master of Science thesis of Dakota Jacobs presented on September 16, 2016

APPROVED:

Major Professor, representing Toxicology

Head of the Department of Environmental and Molecular Toxicology

Dean of the Graduate School

I understand that my thesis will become part of the permanent collection of Oregon State University libraries. My signature below authorizes release of my thesis to any reader upon request.

Dakota Jacobs, Author

TABLE OF CONTENTS

	<u>Page</u>
1 Literature Review	1
2 Materials and Methods	15
3 Chapter One	21
3.1 Introduction	22
3.2 Results	25
3.3 Discussion	28
4 Chapter Two	40
4.1 Introduction	40
4.2 Results	42
4.3 Discussion	44
5 Chapter Three	53
5.1 Introduction	54
5.2 Results	56
5.3 Discussion	57
6 Final Discussion	64
7 References	68

LIST OF FIGURES

<u>Figure</u>	<u>Page</u>
Literature Review:	
1. Figure 1	12
2. Figure 2	13
3. Figure Legends	14
Chapter One:	
1. Figure 1	33
2. Figure 2	34
3. Figure 3	35
4. Figure 4	36
5. Figure Legends	38
Chapter Two:	
1. Figure 1	48
2. Figure 2	49
3. Figure 3	50
4. Figure 4	51
5. Figure Legends	52
Chapter Three:	
1. Figure 1	61
2. Figure 2	62
3. Figure 3	63
4. Figure Legends	64

LIST OF TABLES

<u>Table</u>	<u>Page</u>
1.1 Table No. 1	37

Literature Review

The mammalian endocrine system comprises the strict regulatory network that directs biological processes from conception, throughout development and into adulthood. Processes instigated by endocrine signaling include development of the brain and nervous system, growth and activation of the reproductive axis, and maintenance of metabolic demand. Circulating levels of hormones are low and shift in response to a given stimulus, either environmental or internally, to propagate a unique physiological response, with the longevity of the response being gated by discrete feedback inhibition or stimulation loops. Furthermore, endocrine regulatory mechanisms change throughout development to accommodate the anatomical, physiological, and metabolic maturation of the individual. Considering the criticality of appropriate activation and deactivation of signaling pathways given a particular stimulus, the endocrine system is especially sensitive to endocrine disrupting compounds (EDCs) as these may pose a threat to the coordinated efforts of hormone secreting glands throughout the body to maintain homeostasis.

Of growing interest are EDCs found in the environment, food, and consumer products that impact normal hormonal signaling and biosynthesis. EDCs are a developing public health concern given their effects on male and female reproduction, neuroendocrinology, and breast and prostate cancer. Originally, EDCs were defined as exogenous agents that only interfere with physiological hormonal signaling that are typically responsible for retaining reproduction and development [102]. This definition was derived from the understanding that these compounds bind nuclear hormone receptors including estrogen receptors (ERs), androgen receptors, progesterone receptors and thyroid receptors [102]. However, given the increased attention and subsequent developments in scientific investigation surrounding these deleterious compounds, it is clear that the mechanisms by which EDCs exert their impacts on human health are more divergent and extend beyond

interrupting hormone nuclear receptors. Endocrine disruptors act via non-nuclear steroid receptors, non-steroidal receptors, orphan receptors, and aryl hydrocarbon receptors [102]. Therefore, the definition of EDCs has been redefined to encompass the wide variety of mechanisms by which these compounds can impact human health that supersede endocrine and reproductive systems. Thus, endocrine disrupting compounds are any exogenous substance that modulates physiological hormone and homeostatic mechanisms that allow the organism to appropriately respond and adapt to changing environmental cues [102].

Currently, molecules that are identified as endocrine disruptors are extremely heterogeneous and do not adhere to a particular structural motif that confers an EDC identity. These chemicals include polychlorinated biphenyls, polybrominated biphenyls, and perfluorinated alkyl substances (PFASs) that have halogen substitutions: chlorine, bromine, and fluorine, respectively. Additionally, plastics and plasticizers like bisphenol A (BPA) and phthalates respectively have been identified as having endocrine disrupting characteristics. The classes of compounds listed do not have a shared structural moiety, however, broadly speaking EDCs have halogen substitutions or phenolic substituents that may allow the disruptive role of an agonist or antagonist to steroid receptors.

Some chemicals that demonstrate the capacity to be classified as an EDC have not historically been considered as EDCs. Poly- and perfluorinated alkyl substances (PFASs) were first introduced into consumer products over sixty years ago, including perfluorooctanoic acid (PFOA) and perfluorooctane sulfonate (PFOS) [100] (Figure 2). Due to their incredible thermal stability and unparalleled surface tension reduction capacity, industry professionals employed this remarkable utility in apparel, upholstery, food wrapping, and surface-metal coating to combat water, oil, and grease in consumer products [100]. Due to the resistance to degradation these

chemicals demonstrated, the prevailing consensus among the scientific community was that this particular class of chemicals were inert and therefore do not pose a significant risk to human health if exposed [101]. Such characteristics are detrimental in an environmental context as they become persistent organic pollutants. This persistence manifests as resistance to decay by environmental processes and metabolism within an organism. By 2000, the global environmental and human dispersion for these chemicals became well known to the general public [101]. The Minnesota Mining and Manufacturing company, among the first to both introduce and remove PFOS, agreed to phase out PFOS production by 2002 [101]. Additionally, eight other major U.S. producers have agreed to phase out PFOA by 2015 after the initiation of the PFOA Stewardship Program that seek to completely remove PFOA from industry and environmental compartments [10].

Several PFASs have been identified ubiquitously in environmental compartments including water [1-2], air [3], sediment [4-7] and organisms [8], including various aquatic matrixes: rain [9], snow [10], groundwater [11], tap water [12], rivers [13-15], lakes [16], coastal and offshore seawaters [17-18]. For example, freshwater and seawater samples collected from the River Rhine watershed spanning from Lake Constance to the North Sea, were analyzed for 40 unique PFASs in surface water [19]. The sum PFAS concentration ranged from 0.35 ng/L in the North Sea to 621 ng/L in the River Scheldt, with PFOS and PFOA being major constituents among sampling sites [19]. It is estimated that annual PFAS mass flow into the North Sea from the River Scheldt alone is roughly 2.5 tonnes, with PFOA and PFOS comprising 0.2 and 0.07 tonnes, respectively [19]. PFOS-based products have been phased out since 2002 [20], to be subsequently replaced by short-chained PFASs like perfluorobutanesulfonate, but these data illustrate the persistence and quantity of particular PFAS contaminations that remain in the environment. This abundance and resilience poses a considerable contribution to human exposure, as prolonged

efforts by authorities and industry to phase out the use of PFASs and reduce emissions has not been met with declining environmental concentrations. Indeed, an increasing number of studies show that humans are exposed to a large number of PFASs. Serum collected from young Australians (median age 11 – 13) measured equal or higher levels of several PFASs compared to adults [21]. PFOS has also been measured in children within the United States, with ages ranging from 2 to 12 years old, observed a wide range of concentrations: 6.7 to 515 ng/mL of serum [22]. Exposure routes for children need to be assessed, however one study interrogated the role of breast feeding as a potential route of exposure for young children.

Eight PFASs were identified in whole serum samples collected from Swedish women three weeks postpartum, five chemicals of which were contemporaneously identified in participant-matched milk samples [23]. Highest mean whole serum concentrations were obtained for PFOS, followed by perfluorohexanesulfonate (PFHxS), with 20.7 ng/mL and 4.7 ng/mL, respectively [23]. These particular PFASs were also detected at mean concentrations of 0.201 ng/mL and 0.085 ng/mL, respectively in all milk samples [23]. The total PFAS concentration detected in milk samples was 0.34 ng/mL. Perfluorooctanesulfonamide, PFOA, and perfluorononanoic acid were also detected in blood samples, albeit less frequently in milk samples [23]. Infants would be exposed to this complex mixture of PFAS-contaminated breast milk at approximately 200 ng per day [24]. It is clear that particular EDCs remain in the environment, providing a platform for human exposure, however the consequence of this exposure remains unclear. Several important issues surround EDCs and the impact they impose on human health due to the obligatory reliance on epidemiological studies and sexually dimorphic manifestations of EDC exposure between adult males and females.

Adverse trends in men's health illustrating increased prevalence of testicular cancer [25-26], declining sperm quality [27-28], and increasing frequencies of undescended testis and hypospadias [29], in tandem with a greater need for assisted reproduction are evidenced as being symptoms for an underlying condition: the testicular dysgenesis syndrome (TDS) [30-31]. This syndrome may be increasingly common due to environmental influences, but this epidemiological approach renders the link between TDS and EDC exposures in humans indirect and dated. However, *in utero* or perinatal exposure to exogenous estrogens and anti-androgens in male animal models can lead to hypospadias, undescended testis, low sperm counts, intersex conditions, teratomas, and Leydig cell tumors [32-37]. Furthermore, a similar phenotype to the reduced anogenital distance observed in rats after fetal exposure to some phthalates [38] has recently been reported in an epidemiological report on human male newborns exposed prenatally to the same compounds [39].

In females, the conclusions drawn from EDC exposure and clinical disorders are also weak and indirect, though environmental exposures have been implicated in other conditions related to the female reproductive system including disorders in ovulation and lactation, benign breast disease, breast cancer, endometriosis, and uterine fibroids [40-43]. Endocrine disruption has been investigated since the observations of uncommon vaginal adenocarcinoma in daughters born to women treated with the synthetic estrogen diethylstilbestrol (DES) during pregnancy [44]. Consequently, the mechanism behind DES has been substantiated in rodent models [45], causally linking DES exposure to endocrine disruption. Therefore, robust clinical observations and recapitulative investigations in model systems support the role of some EDCs in male and female reproductive disorders. However, such direct links cannot be generated for the vast array of EDCs present in the environment that may pose a threat to male and female reproductive health,

contributing to a massive controversy associated with connecting EDC exposure to human reproductive dysfunction. Contributors to this controversy are the innate challenges of translating conclusions found in animal models to humans and the complexity of the divergent mechanisms by which EDCs impact human health that may not be mirrored in experimental models.

The genetic framework of an individual can be modulated based on environmental factors, including EDCs that direct the propensity of that individual to develop disease or dysfunction later in adulthood. This concept illustrates the latent effect between initial exposure to EDCs and subsequent tangible outcome. Furthermore, these adverse outcomes are instigated by extremely small doses of EDCs through a chronic exposure window [46]. There is substantial evidence in both rodent models and humans that there may be transgenerational effects of EDCs due to overt mutation or epigenetic modulations. An example of germ-line dependent transmission of epigenetic effects has been observed in a rat model for the fungicide vinclozolin, which increases the likelihood that the next four generations will develop metabolic disorders, tumors, and reproductive dysfunctions [47-52]. Furthermore, EDCs tend to act through divergent mechanisms and have mixed steroidal properties such as both estrogenic and antiandrogenic properties. A single EDC may be metabolized and confer a unique steroidal property from the original parent compound. For example, the estrogen agonist DDT is metabolized into the androgen antagonist DDE [53]. The abundance of metabolizing enzymes in particular tissues where the EDC resides can impact the balance between foreign estrogenic and antiandrogenic molecular properties, which can impact biologically processes that are sensitive to the interplay between androgens and estrogens, like the HPG axis, breast, uterus, cervix, brain and nonreproductive tissues such as bone, muscle and skin. Due to the shared characteristics among EDCs and capacity to interact with hormone receptors, there is not an endocrine system capable of defending against these

compounds, particularly the reproductive axis. Therefore it is incredibly important to understand EDC impact on laboratory animals and humans to better understand how this disruption is directed to reprogramming the HPG axis that may lead to adverse physiological outcomes to interfere with reproductive success.

Mammalian reproductive function hinges on successful transduction of signals through the hypothalamic-pituitary-gonadal (HPG) axis. General characteristics of this central axis and the neuronal modulators of its physiology are relatively conserved among mammalian species. The HPG axis is strictly regulated by neighboring populations of neuronal and non-neuronal glial and astrocytic cell types [54]. The complex intercommunication among hypothalamic cells allows for rigorous control of neuropeptide release within the preoptic area (POA) of the hypothalamus. Axonal terminals extending from cell bodies within the hypothalamus terminate at the median eminence located at the base of the brain to release signals to the hypothalamic-hypophyseal portal vein system connecting the hypothalamus to the hypophysis [54]. This portal vein system allows direct communication between the hypothalamus and hypophysis, allowing regulated secretions of key POA neurons to modulate adeno-hypophysial hormone response efficiently. In a reproductive context, the adeno-hypophysis is stimulated to secrete specific gonadotropins to the circulatory system that facilitate gonadal development and reproductive physiology [55]. These sex steroids suppress hypothalamic secretions to the hypophysis to auto regulate the HPG axis [56]. Sex steroids act to ultimately influence specific hypothalamic neuronal cell types in the POA: gonadotropin-releasing hormone (GnRH) neurons that terminate in the hypothalamic-hypophyseal portal system through the median eminence [56].

GnRH neurons are paramount regulators of HPG axis function, as GnRH release stimulates the adeno-hypophysis to secrete gonadotropins: luteinizing hormone (LH) and follicle stimulating

hormone (FSH) [56]. In males, LH stimulates Leydig cells in the testes to secrete testosterone and acts synergistically with FSH to allow spermatocytes to undergo meiosis to generate viable gametes. In females, LH induces estrogen secretion from follicular granulosa cells, while FSH recruits immature ovarian follicles within the ovary. Typically, elevated blood concentration of testosterone or estrogen provides negative feedback to GnRH neurons. In females, GnRH neurons express estrogen receptor beta ($ER\beta$) that responds to rising estrogen levels by down regulating GnRH secretions, preventing further adenohipophysial gonadotropin-releasing activity. However, GnRH neuron activity requires complex regulation to elicit specific secretion profiles to direct reproductive behavior. This regulation is attained by neighboring neuronal populations within the hypothalamus.

GnRH neuronal perikarya are influenced by two neuroanatomically distinct kisspeptin-releasing nuclei: the anteroventral periventricular (AVPV) and arcuate nuclei (Figure 1) [106]. These nuclei provide regulatory signals to GnRH neurons by kisspeptin, a neuropeptide encoded by the *kiss1* gene expressed highly within the AVPV and arcuate nuclei to modulate reproduction. *Kiss1* is transcribed and translated to kisspeptin in the perikaryon of the neuron and released into extracellular space by vesicular axon transport. Kisspeptin binds to GnRH neuron soma receptors and axon terminals using a kisspeptin receptor, KISS1R. Much like GnRH neurons, AVPV and arcuate neurons are sensitive to rising 17- β estradiol (E_2) levels in the blood. Estradiol effects the transcription activity of *kiss1* in AVPV and arcuate neuronal populations in females, while male rodents lack a sizable AVPV population as they are incapable of generating this surge in gonadotropins. Estrogen receptor alpha ($ER\alpha$) is expressed in the soma of these kisspeptin-expressing neurons, but between the two populations of AVPV and arcuate kisspeptin-secreting

neurons, the transcript level modification of *kiss1* is differentially regulated in several female mammalian species.

Exposure to elevated estradiol causes an increase in *kiss1* expression in the AVPV, whereas a contemporaneous decrease in *kiss1* expression is observed in arcuate nuclei. This differential expression response is only observed in female rodents; male rodents do not express appreciable levels of kisspeptin in the sexually dimorphic AVPV nuclei. However, arcuate *kiss1*-expressing neurons in male rodents exhibit negative feedback from estrogen acting on arcuate neurons, also seen in female rodents [56]. The sexually dimorphic nature of both physiology and anatomy of AVPV kisspeptin neurons is of considerable interest, considering female rodents require GnRH/LH surges to elicit ovulation and AVPV kisspeptin neurons provide positive feedback to GnRH neurons. The AVPV is responsible for the LH timing to overlap with the day of proestrous whereas the arcuate is implicated in regulating the amplitude of the LH surge to potentiate the GnRH signal to the pituitary. This timing could be contingent on AVPV neurons being associated with the suprachiasmatic nucleus via arginine vasopressin receptors gated by estradiol conditions. This differential contributions to the LH surge required to initiate ovulation could be mandated by the unique colocalization of neurokinin B (NKB) and dynorphin A in the arcuate nucleus.

Arcuate kisspeptin neurons colocalize (NKB) and dynorphin neurotransmitters, therefore mammalian arcuate cells have been termed KNDy neurons [57]. This unique colocalization of three neuropeptides to a single neuronal population is restricted to mammalian species, as there are no orthologous neuropeptides expressed by *kiss2* populations in zebrafish [57]. The characteristic kisspeptin system in mammals is absolutely required for proper reproductive function in adults and pre-pubertal mammalian species. An increase in kisspeptin drives the onset of puberty, though the mechanism responsible for this initiation is still unknown. While the

contributions of AVPV and arcuate kisspeptin neurons have been implicated in surge timing and surge amplitude respectively in a fully matured HPG axis, the individual contributions of these two nuclei in the onset of puberty remains unclear.

Pubertal onset is initiated by pulses of GnRH secretion from the hypothalamus to direct the pituitary to secrete LH/FSH to begin the development of secondary sexual characteristics. However, in pre-pubertal rodents this pulsatile secretion of GnRH is quiescent until sexual maturation. A complete mechanism that explains this pulse generation has yet to be developed, but it is clear that kisspeptin plays a pivotal role. Pre-pubertal rodent models that lack a functional KiSS1/KiSS1R system either by mutated *kiss1* or KiSS1R antagonists, fail to initiate puberty as characterized by insufficient blood gonadotropin concentrations [58-59]. Sexually mature rodents that lack kisspeptin or its receptor on GnRH neurons do not have an appropriately regulated HPG axis. Furthermore, the pace of puberty is a complicated function of changing sensitivity of GnRH neurons to circulating levels of estradiol. The gonadostat hypothesis stipulates that GnRH sensitivity to inhibition by estradiol is reduced dramatically in the late juvenile stage of development [60-62]. For instance, a 10-fold increase in estradiol dose is required to completely suppress LH secretion in adults compared to juvenile animals [63]. Conditional ablation of estrogen receptor α (ER α) in kisspeptin neurons in female mice advances puberty onset followed by pubertal maturation arrest in which normal ovulatory cyclicity does not occur [64], therefore the juvenile brake to puberty is lost in this conditional model. Thusly, it is clear that both kisspeptin and estrogenic signaling is paramount for proper pubertal timing and completion to correctly mature the HPG axis. However, it remains unclear how AVPV and arcuate sub-hypothalamic populations act in tandem to mediate estradiol cues to provide kisspeptin signals to direct the onset of puberty.

The prevailing method of investigating *kiss1* expression and regulation utilizes tissue fixation and *in situ* hybridization that makes cellular manipulation *in vivo* difficult. An *in vitro* model would yield rigorous research opportunities to investigate *kiss1* mRNA expression under specific physiological conditions, thereby illustrating the neuroanatomically distinct peptidyl releases that have not yet been elucidated between AVPV and arcuate nuclei. The feasibility of immortalizing specific differentiated neurons *in vivo* by targeting tumorigenesis in transgenic mice has previously been demonstrated by Mellon et. al. [65]. Constitutive expression of Simian virus 40 (SV40) large T-antigen (TAg) driven by GnRH promoters infected into embryonic mice develop proliferative GnRH-expressing tumors [65]. GT1-7 cells that serve as a model system for GnRH expression were derived from these tumors, which are now ubiquitously used in neuroendocrinology research. Applying this method of immortalization in the context of generating separate AVPV and arcuate nucleus model systems is void; the utility of approaching immortalization by targeting tumorigenesis *in vivo* using transgenic mice is not valid if the aim is to distinguish between two hypothalamic regions in culture. Expression of *kiss1* cannot be used to drive the expression of SV40 TAg as this gene is expressed in both populations of interest, therefore an approach that exploits expression of a unique gene among a population would generate a heterogeneous mixture of both AVPV and arcuate nuclei. HPG modulation by AVPV and arcuate nucleus peptidyl release need to be explored separately by generating unique AVPV and arcuate models. This has been achieved and here the utility of these cell lines are explored further in the context of estrogenic signaling and the impact of PFASs as estrogen mimics.

Figures

Figure 1:

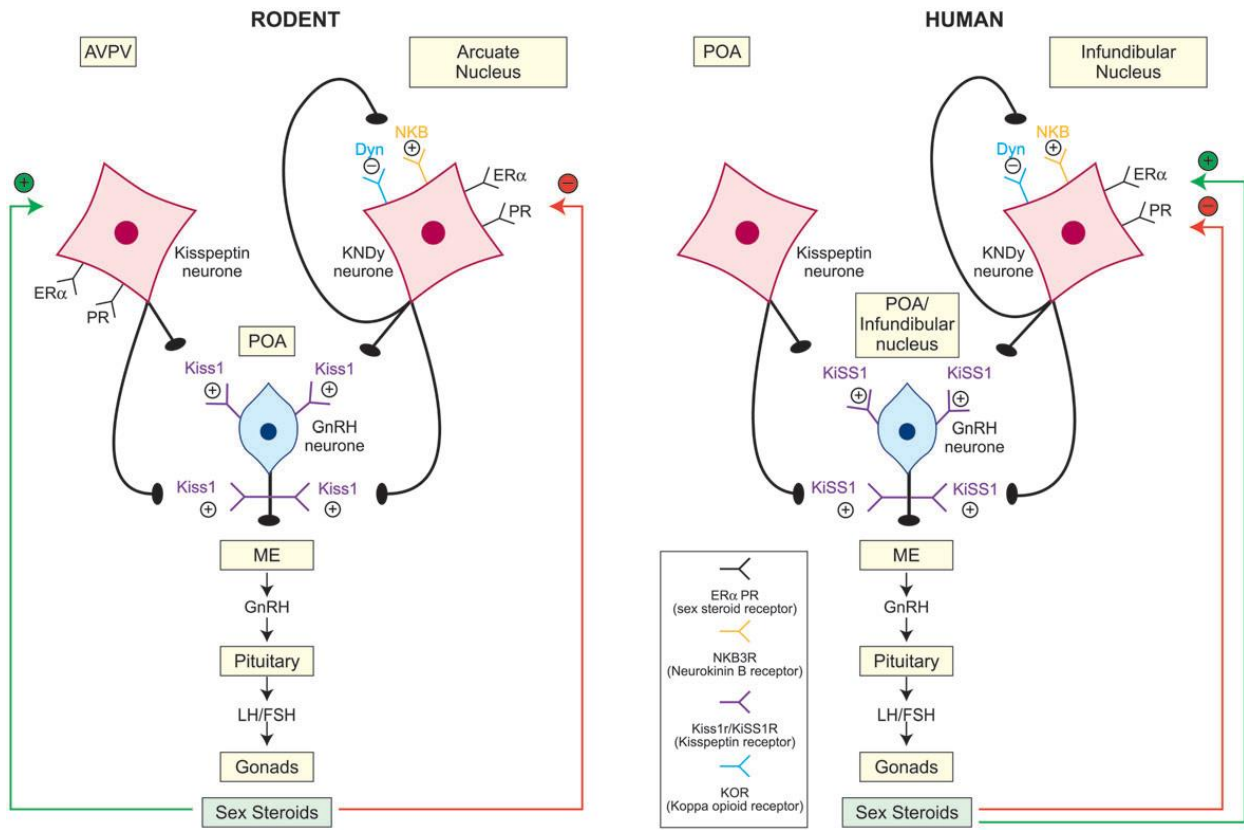
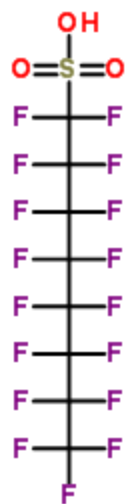


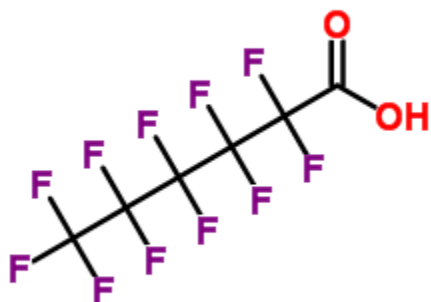
Figure 2:



Perfluorooctanoic sulfonate (PFOS) [103]



Perfluorooctanoic acid (PFOA) [104]



Perfluorohexanoic acid (PFHxA) [105]

Figure Legends

Figure 1:

Schematic depiction of the comparative kisspeptin-GnRH neuronal pathways and the association with the KNDy neurons in rodents and humans. The location of the kisspeptin neuronal populations are species specific, but in both species kisspeptin signals to GnRH neurons through the cognate receptor located at both the soma and axonal terminals. In rodents, kisspeptin neurons are found in the anteroventral periventricular (AVPV) and arcuate whereas in humans they are found in the preoptic area (POA) and infundibular nucleus. Kisspeptin neurons in the infundibular/arcuate nucleus colocalize neurokinin B and dynorphin as well as neurokinin B receptor and kappa opioid peptide receptor that autodynamically regulate kisspeptin secretions with neurokinin B conveying positive feedback and dynorphin conveying negative feedback. Positive (green) and negative (red) feedback at the rodent AVPV and arcuate/infundibular nucleus is mediated by sex steroids, whereas the role of the POA kisspeptin populations in human remains to be appropriately elucidated [106].

Figure 2:

Chemical structures of perfluorooctane sulfonate (PFOS), perfluorooctanoic acid (PFOA), and perfluorohexanoic acid (PFHxA).

Materials and Methods

Animals

Experiments were performed using 9-13 week old female *Kiss1*-GFP (Kiss1-hrGFP) mice. Female transgenic mice were generated by Dr. Carol Elias' lab at the University of Michigan using homologous recombination techniques, derived from Kiss1-hrGFP mice. Female *kiss1*-GFP positive mice were generated from breeding pairs, with all mice housed at the Oregon State University Laboratory Animal Research Center. All mice were maintained on a 12:12 h lighting schedule, with lights on at 6:30 AM, in groups of three to five animals per cage. Access to standard rodent chow and water was *ad libitum*. For sacrifice, mice were briefly anesthetized using an isoflurane chamber followed by cervical dislocation. Care was in accordance with the Institutional Animal Care and Use Committee guidelines and approved by Oregon State University.

Vibratome Preparation

A Microslicer Zero 1 vibratome purchased from Ted Pella was utilized to isolate AVPV and arcuate nuclei explants from adult female *kiss1*-GFP mice. Coronal sectioning was designed based on *in situ* hybridization data provided by the Allen Brain Atlas of an adult male mouse. The vibratome specimen mount was placed in a cold slurry of ice and water before mouse anesthesia and the slurry was maintained throughout the procedure. Two stacked agar blocks were anchored with Loctite to the specimen plate to support the brain. Sectioning protocol was followed as described by the vibratome manual.

Tissue Extraction, Explant Collection and Plating

Complete brain extraction was performed post isofluorane anesthesia followed by standard pinch test and cervical dislocation. The brain was quickly removed from the skull under aseptic conditions. A small portion of the cerebellum was truncated using a sterile razor blade to allow a flat surface for anchorage on the vibratome specimen plate. The caudal region of the brain was fixed to the center of the specimen plate to orient the rostral olfactory bulb upward, with Loctite placed in front of the stacked agar blocks. Upon solidification of the Loctite, the agar blocks and specimen were submerged in chilled artificial cerebral spinal fluid with calcium chloride (recipe described fully by Sue Moenter at the University of Michigan). Two 2500 μ m rostral-caudal cuts were made, followed by a 500 μ m cut containing the AVPV nucleus of the hypothalamus. Sagittal and transverse trims were made on the AVPV nucleus explant, which was then placed in a covered 1.5mL Eppendorf tube containing 1 mL serum free Dulbecco's Modified Eagle Medium (DMEM) with 1% collagenase. Another 1000 μ m cut was made to expose the arcuate nucleus. A final 1000 μ m cut was made to isolate the arcuate, followed by sagittal and transverse trimming, followed by placement into a covered 1.5mL Eppendorf tube containing 1mL serum free (SF) DMEM with 1% collagenase. AVPV and arcuate nuclei explants were enzymatically digested for 45 minutes on a shaker plate at 37°C before plating. Collagenase was deactivated by addition of fetal bovine serum (FBS) to each AVPV nucleus and arcuate sample to yield a solution of 20% FBS DMEM. In a 24-well plate, approximately 100 μ L of AVPV or arcuate digest was added to six individual wells for a single explant. The final volume was brought up to 1mL with a solution of 20% FBS DMEM. Cultured neurons were treated with penicillin, streptomycin, and gentamicin for the duration of the experiment.

Plasmid Isolation and immortalization

All plasmids were delivered in a bacterial stab from Addgene and stored at 4°C for one week before each individual plasmid was cultured and purified. Agar plates were inoculated with ampicillin-resistant bacteria and cultured overnight at 37°C, and subsequently grown in liquid culture. Qiagen maxiprep yielded purified plasmids, as confirmed by restriction digestion analysis. Four separate plasmids were isolated: (1) pLenti CMV/TO SV40 small and large T-antigen (w612-1) (Addgene plasmid #22298); and (2) pMDLg/pRRE (Addgene plasmid #12251), (3) pRSV-Rev (Addgene plasmid #12253), and (4) pMD2.G (Addgene plasmid #12259). Human embryonic kidney (HEK) 293T cells were grown to 60-70% confluent cell density overnight in 37°C and 5% CO₂ incubation in a T25 flask in 10% FBS DMEM with penicillin, streptomycin, and gentamicin. Media change occurred once, one hour before transfection with lentiviral plasmids. Transfection of HEK 293T cells was performed in adherence to the Lipofectamine 3000 (Life Technologies) protocol with RPMI replacing Opti-MEM medium to dilute 7.5µL Lipofectamine 3000 and plasmid DNA for a 6-well volume. Two micrograms of plasmid DNA in a 4:2:2:1 ratio was added, with four parts SV40 TAg plasmid, two parts pMDLg/pRRE plasmid, two parts pMD2.G plasmid, and one part pRSV-Rev. The DNA-lipid complex was incubated at room temperature for 5 minutes after gentle mixing, then added to HEK 293T cells. HEK 293T cells were incubated with lentiviral DNA for 12 hours prior to collection. The complete virus was filtered into a 15mL conical tube using a 45µm syringe filter. Filtered virus-containing media was aliquoted to two 1mL microfuge tube, one for the AVPV and one for the arcuate. Two microliters of Polybrene (4µg/µL) was added to each 1mL aliquot of complete virus. Four weeks following primary culture harvest, the media in each well of AVPV and arcuate nucleus in 24-well plates was aspirated and replaced with 200µL of viral supernatant and 800µL SF DMEM. Approximately 16 hours after initial infection, virus-

containing media was aspirated and cells from each well were resuspended in 20% FBS DMEM with penicillin, streptomycin and gentamicin.

Fluorescence-Activated Cell Sorting (FACS)

One month after immortalization, 10cm plates of AVPV and arcuate nuclei were washed with 1X PBS and treated with 2mL of TrypLE in 5% CO₂ at 37°C for 5 minutes prior to resuspension in 20% FBS DMEM. Samples were transferred to sterile 15mL conical tubes and centrifuged for two minutes at 1000 rpm. Supernatants from both samples were aspirated and the cell pellet was resuspended in 1X PBS. FACS was performed with a Beckman Coulter (Brea, California) MoFlo XDP using a solid state blue laser with excitation at 488 nm. Cells were sorted based on positive fluorescence signal in the green channel (530 nm PMT detector with a 40 nm bandpass filter) gated on a scatter to exclude cell debris in a bivariate histogram. Cells within the gate were collected in 1mL of 10% FBS DMEM. AVPV cells were re-plated in three wells of a 12-well plate and arcuate cells were plated in four wells of a 12-well plate. KTaV-3 and KTaR-1 cells were expanded after gene screening.

Transcript Characterization

Total RNA was harvested from individual confluent 3cm plates of AVPV and arcuate neuron samples using TRIzol. Purified RNA was reverse transcribed to cDNA using a High Capacity cDNA Reverse Transcription kit (Applied Biosystems) to be used for PCR. For each reaction, 2µL of 10X RT buffer, 0.8µL 25X dNTP Mix (100mM), 2µL 10 RT random primers, 1µL Multiscribe reverse transcriptase, and 4.2µL of nanopure water was added to 1µg of RNA in a 10µL volume. Several gene sequences were targeted to test efficacy of immortalization and characterize

expression of specific genes in each respective neuronal population. Primers were designed based on published sequences for mouse kisspeptin (*kiss1* NM_178260), prodynorphin (*pDyn* NM_001286502), and neurokinin B (*Tac2* NM_001199971). Table 1 details the gene of interest, primer sequence, and amplicon size. PCR reactions contained a total volume of 10 μ L: 1 μ L of converted cDNA, 1 μ L of 10 μ M primer mix, 3 μ L of nanopure H₂O, and 5 μ L of Gotaq Green Master Mix. PCR products were visualized via electrophoresis on 1 – 2% agarose gels containing ethidium bromide. Transcript abundance was characterized with standard RT-PCR.

Estrogen Treatment

A confluent 10cm plate of immortalized KTaV-3 neurons was split to 3cm dishes at a cell density of 1.87x10⁵ cells per plate; this was repeated for the immortalized KTaR-1 neurons. Except the 0hr, each plate was serum synchronized with 50% FBS DMEM two hours prior to collection. After two hours, cell media was replaced with either SF media containing 1X PBS as control or SF media containing 25pM estradiol. Next, 500 μ L of media was collected every four hours from both KTaV-3 and KTaR-1 treatment conditions simultaneously, 500 μ L of TRIzol was collected at each time point for each treatment condition for KTaV-3 and KTaR-1 neurons. RNA was isolated from TRIzol and converted to cDNA; media samples were used to detect kisspeptin secretion by ELISA.

Kisspeptin ELISA

Media kisspeptin levels from AVPV and arcuate neuron samples were quantified by ELISA (LifeSpan BioSciences, Catalog No. LS-F11879) with a sensitivity range of 78-5000pg/mL, and assay CV < 3.6%. Standard curve derivation and sample preparation was performed as dictated by the ELISA user manual.

PFOS, PFOA, and PFHxA Treatment

A confluent 10cm plate of immortalized KTaV-3 neurons was split to 3cm dishes at a cell density of 1.87×10^5 cells per plate; this was repeated for the immortalized KTaR-1 neurons. Plates were replaced with SF media containing 25 fM, 25 pM, 25 nM PFOS. This was repeated for PFOA and PFHxA and DMSO control. After 4 hour incubation in these treatment conditions, 500 μ L of TRIzol was collected for each treatment condition for KTaV-3 and KTaR-1 neurons. RNA was isolated from TRIzol and converted to cDNA.

Chapter One: Evaluation of immortalized AVPV- and arcuate-specific neuronal Kisspeptin cell lines to elucidate potential mechanisms of estrogen responsiveness and temporal gene expression.

Abstract

Ovulation requires preovulatory surges of gonadotropin-releasing hormone (GnRH) from neurons in the preoptic area of the hypothalamus, initiated by elevated ovarian estradiol (E₂). Rising estradiol activates a subset of sexually dimorphic kisspeptin (Kiss-1) neurons in the female, located in the anteroventral periventricular nucleus (AVPV). Conversely, estradiol negative feedback is mediated by a separate population of kisspeptin neurons in the arcuate nuclei. Kiss-1 is an obligatory regulator of GnRH release *in vivo*, and development of the kisspeptin system is critical for pubertal initiation. To elucidate how differential responsiveness to estradiol is mediated in these two populations, we generated two kisspeptin-releasing cell lines from a *kiss1*-GFP post-pubertal female mouse. These independent cell models recapitulate *in vivo* differential responsiveness to estradiol, with KTaV-3 (AVPV model) cells demonstrating increased *kiss1* expression after a 4 hour incubation in estradiol. In KTaR-1 (arcuate) cells, *kiss1* was suppressed after a 4 hour incubation with low concentrations of estradiol. Baseline expression of estrogen receptor α (*esr1*) differs significantly between KTaV-3 and KTaR-1 cells, with KTaR-1 cells demonstrating higher basal expression of *esr1*. As a function of dose, KTaV-3 *kiss1* expression increases in response to estradiol, with a reduction from peak response at higher doses (>50pM E₂). In contrast, KTaR-1 *kiss1* expression is attenuated across a low estradiol dose range, returning to control levels at 25pM and above. Additionally, the transcription quantification of core clock genes *bmal1* and *per2* show distinct antiphase patterns in KTaV-3 cells, regardless of estradiol

treatment. Conversely, KTaR-1 antiphasic transcriptional activity of *bmal1* and *per2* is only present in the absence of estradiol, and estradiol application induced a possible antiphase-delay. Strikingly, 25pM E₂ treatment induces a circadian rhythm of *kiss1* expression only in KTaV-3 cells, one that is not observed in control conditions. Further exploration into estradiol responsiveness will reveal mechanisms responsible for the differential expression pattern demonstrated *in vivo* between these cell types.

Introduction

The neuropeptide kisspeptin (Kiss-1) provides critical afferent stimulation to gonadotropin-releasing hormone (GnRH) neurons in the mammalian hypothalamus. In females, Kiss-1 synthesis and release are orchestrated by two neuroanatomically distinct nuclei: the sexually-dimorphic anteroventral periventricular (AVPV/R3PV) and the arcuate nuclei. The gene encoding this peptide, *kiss1*, is expressed in both locations in female rodents, but expression is differentially regulated by estradiol at these sites, inhibiting *kiss1* expression in the arcuate nuclei during diestrus while stimulating expression in the AVPV on proestrus. The requirement for kisspeptin-GnRH communication is demonstrated in animals with deactivating mutations in *gpr54/kiss1r*, the cognate receptor for kisspeptin. In humans, a loss of this signaling is linked to hypogonadotropic hypogonadism and an absence of pubertal onset. In mice, *kiss1* [66, 67] and *gpr54* [68, 69] knockouts exhibit hypogonadism and infertility. Exogenous administration of kisspeptin has the capacity to restore fertility in rodent *Kiss1* KO models by increasing GnRH secretion as well as promoting pubertal onset [70-72]. In humans, kisspeptin has been shown to induce a surge of luteinizing hormone (LH) and subsequent egg maturation, illustrating its GnRH-stimulating capacity [73]. Conversely, binding of Kiss1R/GPR54 by the antagonist p234 delays pubertal onset

in mice [74]. From these observations, it is clear that the integration of these signals in the brain is paramount for proper reproductive axis maturation and normal GnRH secretion.

The preovulatory GnRH/LH surge is contingent on rising estradiol and is gated by circadian oscillators in both the suprachiasmatic nucleus (SCN) [75-77] and GnRH neurons [78-80], confining the surge to a temporally-defined window on the afternoon of proestrus. Previous studies have identified a possible mechanism by which the SCN may modulate GnRH neuronal activity via AVPV neurons [81, 82], particularly *kiss1*-expressing subpopulations. AVPV *kiss1* and *c-fos* coexpression peak concurrently with an LH surge in OVX+E₂ treated mice, suggesting a circadian pattern may be elicited following estradiol exposure [83]. This estradiol-dependent rhythmicity may occur in coordination with rhythmic increases in GnRH neuronal sensitivity to Kiss-1 only in the presence of estradiol, mediated by temporally regulated increases in Kiss1R/GPR54 abundance [80]. AVPV Kiss-1 neurons are directly innervated by SCN AVPergic neurons by a monosynaptic pathway [84], thereby affording AVPV neurons the capacity to modulate GnRH neuron activity by integrating both hormonal feedback and circadian signals. The significance of endogenous circadian clock function or sensitivity to SCN-derived signals in arcuate Kiss-1 neurons remains unclear, as an analogous monosynaptic pathway has not been identified in this cell population.

AVPV and arcuate kisspeptin signaling to GnRH neurons has been shown to be required to initiate puberty, with the relative importance of these hypothalamic nuclei explored *in vivo*. AVPV-specific contributions were revealed by infusion of a kisspeptin-specific antibody into the preoptic area (POA), which diminished LH surge amplitude and suppressed estrous cyclicity [85]. Arcuate neurons are implicated in GnRH pulse generation, and many have been found to co-express neurokinin B (NKB) and the opioid dynorphin A (Dyn) [86]. Stereotaxic-injection of

AAV-associated viral constructs expressing *kiss1* antisense oligos (rAAV-Kp-AS) into the AVPV delays vaginal opening by 3.4 days and first estrous by 3.8 days, indicating the requirement of this neuropeptide in initiating puberty and completing HPG axis maturation [87]. Similar kisspeptin expression knockdown in arcuate nuclei does not influence pubertal onset, yet still results in abnormal estrous cyclicity and dampened LH pulse frequency and amplitude [87]. While these observations illustrate the division between LH pulse and surge generation as regulated by arcuate and AVPV neurons, respectively, many of the cellular and molecular mechanisms underlying Kiss-1 neuronal population-specific differences in activity and sensitivity to sex steroids are unclear. Recent progress has been made to generate immortalized cell lines from isolated female mouse hypothalamus as a model for AVPV kisspeptin-releasing neurons [88, 89]. Quantitative PCR analysis demonstrates *kiss1*, *esr1*, and *pgr* expression in immortalized mHypoA51 cells [90]. While clearly valuable models, some cell lines used were not derived via initial selection for Kiss-1 [88], thus specificity of these existing cell models is unclear.

To better address mechanisms underlying differences in estradiol-responsiveness between arcuate and AVPV Kiss-1 neurons in females, we have generated and characterized two novel immortalized *in vitro* cell models, KTaR-1 and KTaV-3, derived from arcuate and AVPV nuclei, respectively, from an adult female mouse hypothalamus. We have probed these cell lines and determined that they maintain many of the properties of Kiss-1 neurons described *in vivo*, particularly in terms of differential estradiol-responsiveness. We report that the specific directional expression changes in *kiss1* in response to estradiol are retained in these lines, and we explore both dose- and time-dependency of estradiol exposure on these effects. These studies also reveal differential basal expression levels of *esr1/esr2*. Additionally, we explore the dose effects of

estradiol on *kiss1* expression between KTaV-3 and KTaR-1 cells, as well as addressing the potential role of endogenous circadian oscillators in each cell type.

Results

Expression profiles of immortalized KTaV-3 and KTaR-1 neuronal cells.

Typical morphological characteristics expected to be demonstrated by neuronal cell lines were observed in both KTaV-3 and KTaR-1 lines, including the appearance of normal processes and neurite extensions (**Figure 1A and C**). GFP fluorescence driven by *kiss1* promoter activation was observed in both cell lines (**Figure 1B and D**) shortly after FACS sorting. The neuronal phenotype of these cells is further supported by an absence of expression of the glial-specific gene, glial fibrillary acidic protein (*gfap*, **Figure 1E**). Importantly, KTaV-3 and KTaR-1 both express *kiss1* (**Figure 1F**), whereas *tac2* (**Figure 1G**) and *pdyn* (**Figure 1H**) are robustly expressed only in KTaR-1 cells, suggesting that these cells are representative of Kiss-1 neurons *in vivo*. Real-time qPCR analysis revealed a slightly higher baseline expression of *kiss1* in KTaR-1 cells vs. KTaV-3 cells in 10% FBS growth media, though not statistically significant (**Figure 1I**). Furthermore, baseline expression of *esr1* is significantly elevated in KTaR-1 (3.66 ± 0.42 ; p-value < 0.05) compared to KTaV-3 cells, while *esr2* expression did not vary between the two cell lines (**Figure 1J**).

KTaV-3 and KTaR-1 cells recapitulate in vivo differential responsiveness to estradiol of kiss1 expression and KISS-1 peptide secretion.

To determine if differential responsiveness of arcuate- and AVPV-derived cells to estradiol exposure is retained in KTaR-1 and KTaV-3 cells, *kiss1* expression was evaluated by qPCR

following treatment with 17 β -estradiol. Strikingly, KTaV-3 cells exhibited a ~6-fold increase in *kiss1* expression following a 4h exposure to 25.0 pM E₂ (6.3 ± 0.24 ; p-value < 0.005) and a subsequent peak after 24h (3.8 ± 0.55 ; p-value < 0.05) (**Figure 2A**). In contrast, a 4h treatment with 5.0 pM E₂ repressed *kiss1* expression in KTaR-1 cells by ~60% (0.40 ± 0.13 ; p-value < 0.005) (**Figure 2B**). Notably, KTaR-1 cells maintained in serum-free (SF) media containing 1X PBS vehicle visibly increased *kiss1* expression after 4 h (3.16 ± 1.44), demonstrating that the removal of residual estradiol present normally in FBS diminishes the repressive effects of estradiol on *kiss1* expression only in KTaR-1 cells.

Differential baseline expression of *kiss1* observed in each cell line was corroborated by commensurate levels of KISS-1 peptide released into the media during static incubation, as measured via ELISA (**Figure 2C**), with KTaR-1 cells releasing more KISS-1 (55.1 ± 11.8 pg/mL) in normal growth conditions than KTaV-3 cells (23.0 ± 4.6 pg/mL). Additionally, perfusion of both cell types on Cytodex 3 beads revealed that KTaR-1 and KTaV-3 cells secrete measurable levels of KISS-1 in this format, and that secretion of KISS-1 was stimulated by exposure to 50 pM E₂ in perfusion buffer in KTaV-3 cells after 12h (vehicle 19.25 ± 1.75 , vs 50 pM E₂ 63.5 ± 6.45 ; p-value < 0.001), while repressed in KTaR-1 cells under the same conditions (vehicle 66.9 ± 2.65 vs 50 pM E₂ 38.3 ± 2.04 ; p-value < 0.001).

Estradiol modulation of kiss1 expression occurs within a narrow dose range

To further define which doses of 17 β -estradiol elicit maximal stimulation and repression of *kiss1* expression in KTaV-3 and KTaR-1 cells, respectively, 3cm plates of cells were treated with estradiol doses ranging from 2.0-100.0 pM. RNA was collected in TRIzol, isolated, and analyzed for changes in *kiss1* expression as above. All doses of estradiol stimulated *kiss1* expression in

KTaV-3 cells, with significant elevations observed at 5.0 and 10.0pM E₂, (5 pM E₂ 5.34 ± 1.38 vs 10 pM E₂ 5.84 ± 2.08) and a peak increase of ~9-fold at 25.0 pM E₂ (9.07 ± 4.44; p-value < 0.01, **Figure 3**). *Kiss1* stimulation diminished at higher 50.0-100.0 pM doses of estradiol in this cell line. In KTaR-1 cells, 2.0-10.0 pM doses elicited maximal repression (2 pM E₂ 0.57 ± 0.09, vs 5pM E₂ 0.38 ± 0.1, vs 10pM E₂ 0.41 ± 0.14; p-value < 0.01), though repression was lost at higher (25.0-100.0pM) doses of estradiol (**Figure 3**).

Estradiol modulates differential temporal expression patterns of kiss1 in each cell line.

To explore temporal changes in *kiss1* expression in these two cell types following estradiol exposure, we converted RNA to cDNA from samples harvested every 4 hours for 24 hours following either vehicle (PBS) or 17β-estradiol treatment, and examined expression profiles of core circadian clock genes. Quantitative PCR analysis revealed normal antiphasic rhythms of *bmal1* (peak at 12hr following serum synchronization) and *per2* (nadir at 12-16h) in KTaV-3 cells in both the presence and absence of 25pM E₂ (**Figure 4A**). While *kiss1* expression levels did not change appreciably in control-treated KTaV-3 cells, 25.0 pM E₂ treatment elicited significant increases in *kiss1* expression at 4hr and 24 hours (6.3 ± 0.24; p-value < 0.005 and 3.8 ± 0.55; p-value < 0.05) (**Figure 4C**). In contrast, serum synchronized KTaR-1 cells treated with vehicle demonstrated antiphasic patterns of *bmal1* and *per2* expression, while treatment with 5.0 pM E₂ appeared to phase-delay the expression peaks of both genes (**Figure 4B**). Additionally, 5.0 pM E₂ treatment repressed *kiss1* expression at 4h (0.40 ± 0.13; p-value < 0.005), while inducing a peak at 20h (4.06 ± 0.6). This increase in *kiss1* expression was also noted in serum-synchronized, vehicle-treated KTaR-1 cells at 20h (4.14 ± 2.82), preceded by a robust increase in *kiss1* expression at 8h (5.95 ± 2.83) (**Figure 4D**).

Discussion

A consensus view derived from several earlier studies performed *in vivo* posits a requirement for *kiss1* expression in HPG axis maturation, pubertal progression, and adult reproductive physiology. In this model, dynamic changes in GnRH neuronal secretion are mediated by afferent stimulation through AVPV and arcuate kisspeptin release in the mammalian hypothalamus. While several *in vivo* approaches have characterized the differential responsiveness of these two *kiss1*-expressing nuclei to estradiol exposure, molecular mechanisms underlying this differential regulation remain unclear. We generated two kisspeptin-synthesizing and -secreting cell lines to better assess direct effects of estradiol on these neurons to probe underlying molecular mechanisms and explore temporal patterns of gene expression.

Validation of immortalized cell lines

Here we described two neuronal cell lines representative of AVPV (KTaV-3) and arcuate (KTaR-1) nuclei derived from a fully differentiated transgenic adult female mouse hypothalamus using *kiss1*-GFP selection. Clonally expanded KTaV-3 and KTaR-1 cells from pooled clones lack *gfap* expression, suggestive of a neuronal phenotype, and express *kiss1*. It should be noted that the non-specific binding demonstrated by KTaR-1 and GT1-7 controls is not illustrative of a glial genotype as the expected product size (224 bp) is not recaptured in any of the neuronal models (KTaV-3, KTaR-1, or GT1-7). Furthermore, co-expression of *tac2* and *pdyn* is observed in KTaR-1 neurons, supporting these cells as an accurate representation of arcuate *kiss1*-expressing neurons. KTaV-3 neurons do not express appreciable levels of either *tac2* or *pdyn*, results which agree with other recently published immortalized cell models (26). Similar to this very recent study, estradiol-induced expression changes in *kiss1* were observed in KTaR-1 and KTaV-3 that recapitulate *in*

in vivo results in terms of differential responsiveness, such that KTaV-3 neurons increase expression of *kiss1* following estradiol exposure, whereas KTaR-1 neurons constitutively repress *kiss1* expression in estradiol treatment conditions. In the current study, larger effects of estradiol on *kiss1* expression were noted in comparison to the previous study (26), potentially resulting from administration of physiological estradiol dose ranges. We observed maximal stimulation of *kiss1* expression in KTaV-3 cells following 25.0 pM E₂, with a blunted stimulation at higher doses, comparable to those used in the previous study. Similarly, 5.0-10.0 pM E₂ exerted maximal repression of *kiss1* expression in KTaR-1 cells, with a lack of repression observed at higher doses. These results suggest that Kiss-1 neurons in both neuronal subpopulations are sensitive to a relatively narrow concentration range of ovarian estradiol, such that lower doses can exert robust negative feedback influence on Kiss-1 neurons in the arcuate, while higher (25.0 pM) concentrations approximating proestrus afternoon levels exert maximal stimulation on AVPV Kiss-1 neurons. These results suggest that the effects of E₂ on *kiss1* expression are mediated via direct action of the steroid hormone on Kiss-1 neurons, and do not require innervation from other neuronal cell types for this observed modulation in *kiss1* expression. KTaR-1 cells return to baseline *kiss1* expression (and somewhat higher) levels at exposure to 25.0-100.0 pM E₂, suggesting the possibility that arcuate Kiss-1 neurons may not be appreciably inhibited during proestrus and may potentially contribute to GnRH surge secretion, although this will require future verification.

Exploring estradiol modulation of temporal kiss1 expression patterns

While many previous *in vivo* studies demonstrated that ovarian estradiol elicits changes in expression of *kiss1* and other genes, a few have suggested that *kiss1* may exhibit a circadian

expression pattern in the presence of elevated estradiol only [83]. In the current study, we found that *kiss1* expression patterns over time were significantly altered by exposure to 25 pM E₂ in KTaV-3 cells, in contrast with a low and arrhythmic pattern observed under estradiol-free conditions. These results support the previous *in vivo* study, which did not address patterns of core clock gene expression. We found that rhythmic expression of core clock genes *per2* and *bmal1* is observed in serum-synchronized KTaV-3 cells regardless of estradiol treatment condition, suggesting that rhythmic expression of *kiss1* at 4 h and 24 hours is not mediated by changes in circadian clock oscillations, but rather at the point of coupling intracellular clock function with *kiss1* expression following estrogen receptor (ER) activation. A similar effect of estradiol on gene expression rhythms was previously suggested in GnRH neurons *in vitro*, as *gpr54* expression in GT1-7 cells was shown to be rhythmically expressed only in the presence of elevated estradiol [80]. In contrast, while vehicle-treated KTaR-1 cells exhibited analogous core clock gene patterns, this expression pattern was shifted by low-dose (5.0 pM) E₂, suggesting that in contrast to the AVPV, steroid milieu can effect intracellular oscillators. A peak of *kiss1* expression was observed at 20 h following serum-synchronization regardless of estradiol treatment in KTaR-1 cells (though not significantly), suggesting that the potential clock-*kiss1* coupling observed in the AVPV does not occur in the arcuate, but that rhythms of *kiss1* may be influenced by *per2* expression levels irrespective of estrous cycle stage. The robust increase in *kiss1* expression at 8 h in KTaR cells is likely the result of the removal of estradiol present in serum, which was observed earlier in Figure 2B. Together these results suggest that absence or presence of estradiol appears to exert a greater effect than intracellular oscillators on changes in *kiss1* expression in the arcuate nuclei.

The KTaV-3 and KTaR-1 cell models, based on recapitulation of *in vivo* gene expression responsiveness to estradiol, appear to accurately represent AVPV and arcuate nuclei, respectively.

KTaV-3 cells display core clock gene oscillations irrespective of vehicle or estradiol treatment conditions, whereas estradiol modulates circadian clock rhythms observed in KTaR-1 cells. These data suggest that *kiss1* expression modulation in AVPV nuclei after estradiol exposure may be coupled to the circadian oscillations of *bmal1* and *per2*, whereas the repression of *kiss1* after estradiol in the arcuate is the predominant immediate effect, and may occur independently of clock alteration. The role of endogenous circadian oscillators in Kiss-1 neurons *in vivo* is currently unclear, but the current results reinforce earlier studies suggesting that rhythmic patterns of *kiss1* expression in the AVPV are found only in the presence of estradiol. The AVPV are bilateral nuclei innervated by the nearby SCN, which acts as the brain's central circadian synchronizer. Neuropeptide release, including AVP and VIP, has been demonstrated to exert effects on AVPV neurons [92-95]. A very recent study indicates that AVP-stimulated activity of AVPV Kiss-1 neurons requires the presence of estradiol, although no rhythm of activity was noted [96]. It is possible that estradiol gates a threshold expression level of V1AR required for Kiss-1 secretory responsiveness to AVP, while expression of *kiss1* is coupled to an internal clock. Future studies will explore these possibilities further. These cell models will hopefully provide valuable tools to delineate the influences of estrogenic feedback mechanisms in AVPV and arcuate models required to regulate HPG axis maturation and function.

Acknowledgements

We would like to thank Dr. Carol Elias of the University of Michigan for her contribution of the transgenic *kiss1*-GPF mice utilized in this study. We would also like to thank Sam Bradford of the flow cytometry core at Oregon State University for performing the fluorescent activated cell

sorting to generate these lines. Lastly, we would like to thank Cheri Goodall for invaluable technical assistance and advice.

Figures

Figure 1:

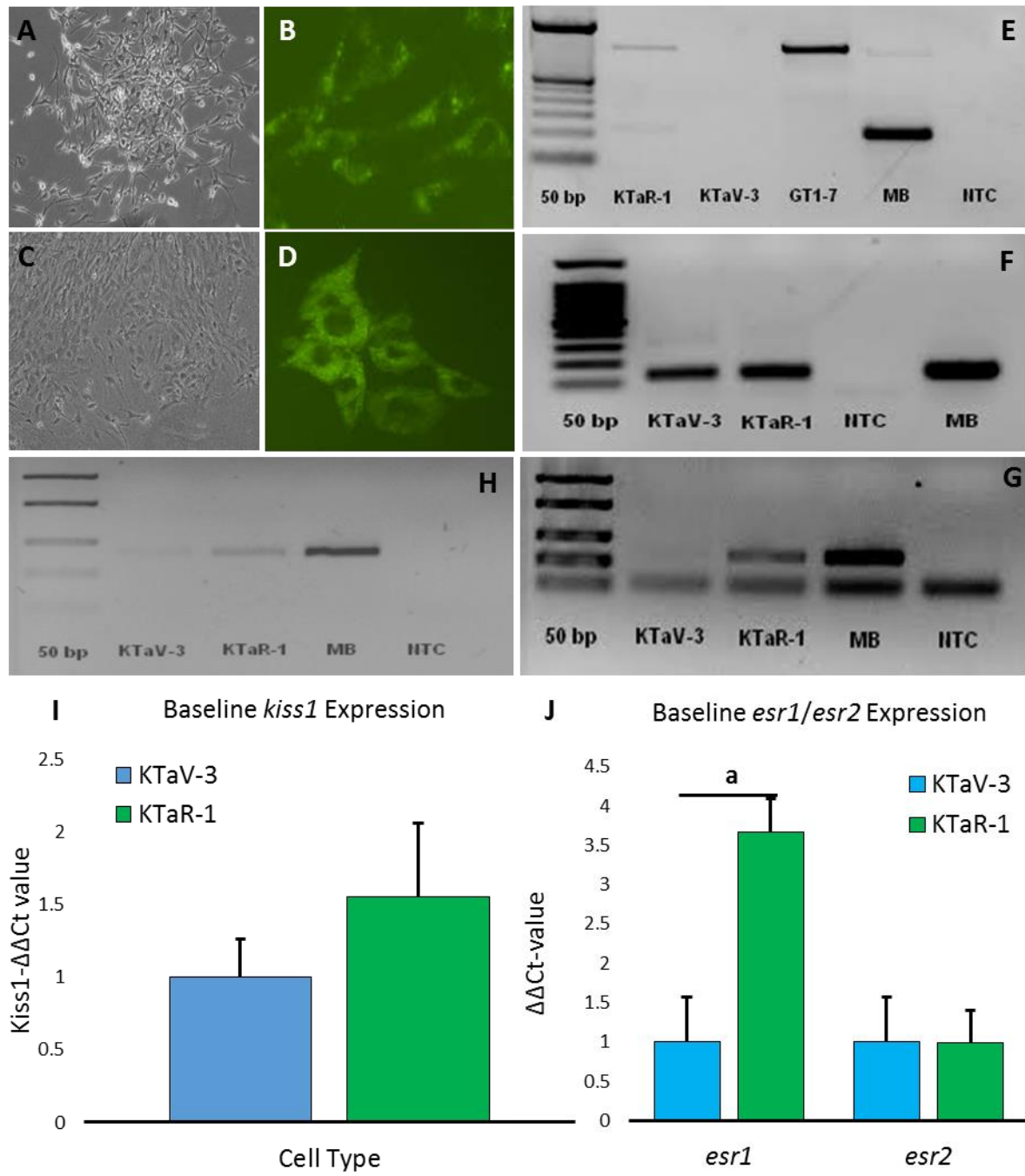


Figure 2:

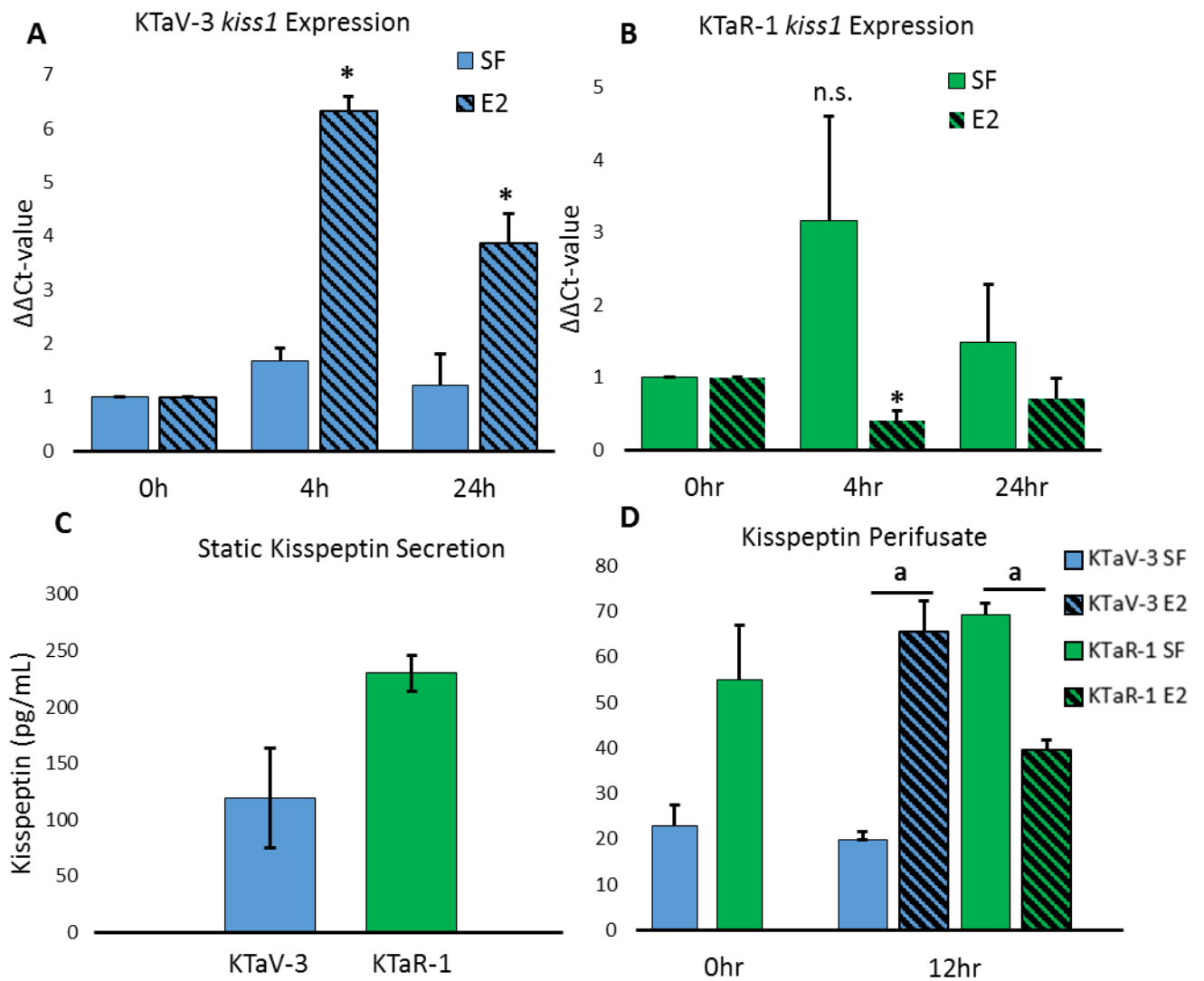


Figure 3:

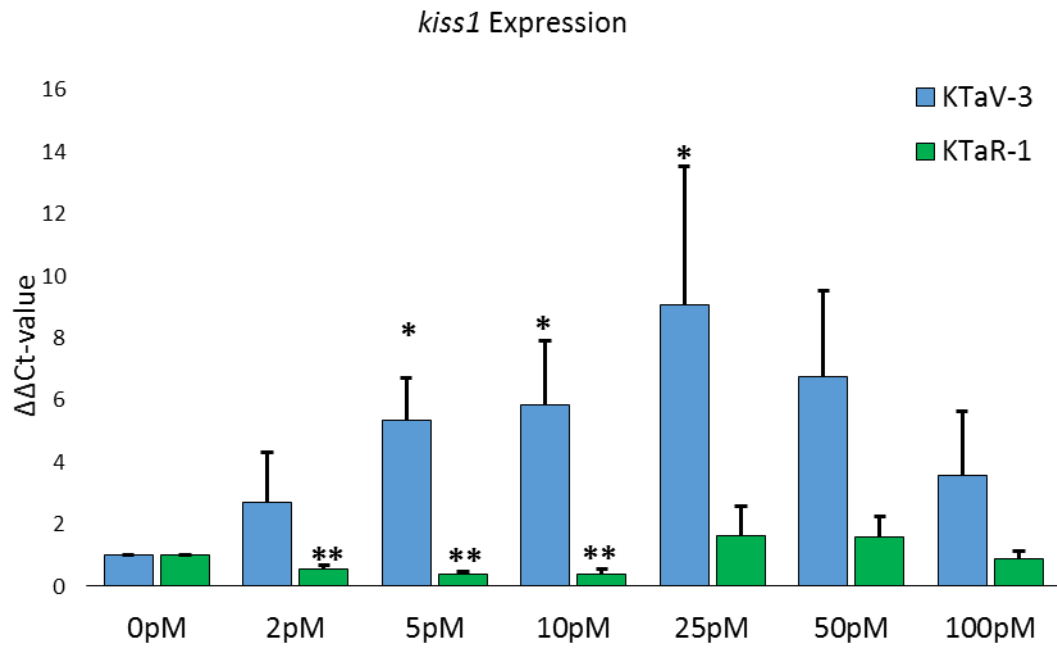


Figure 4:

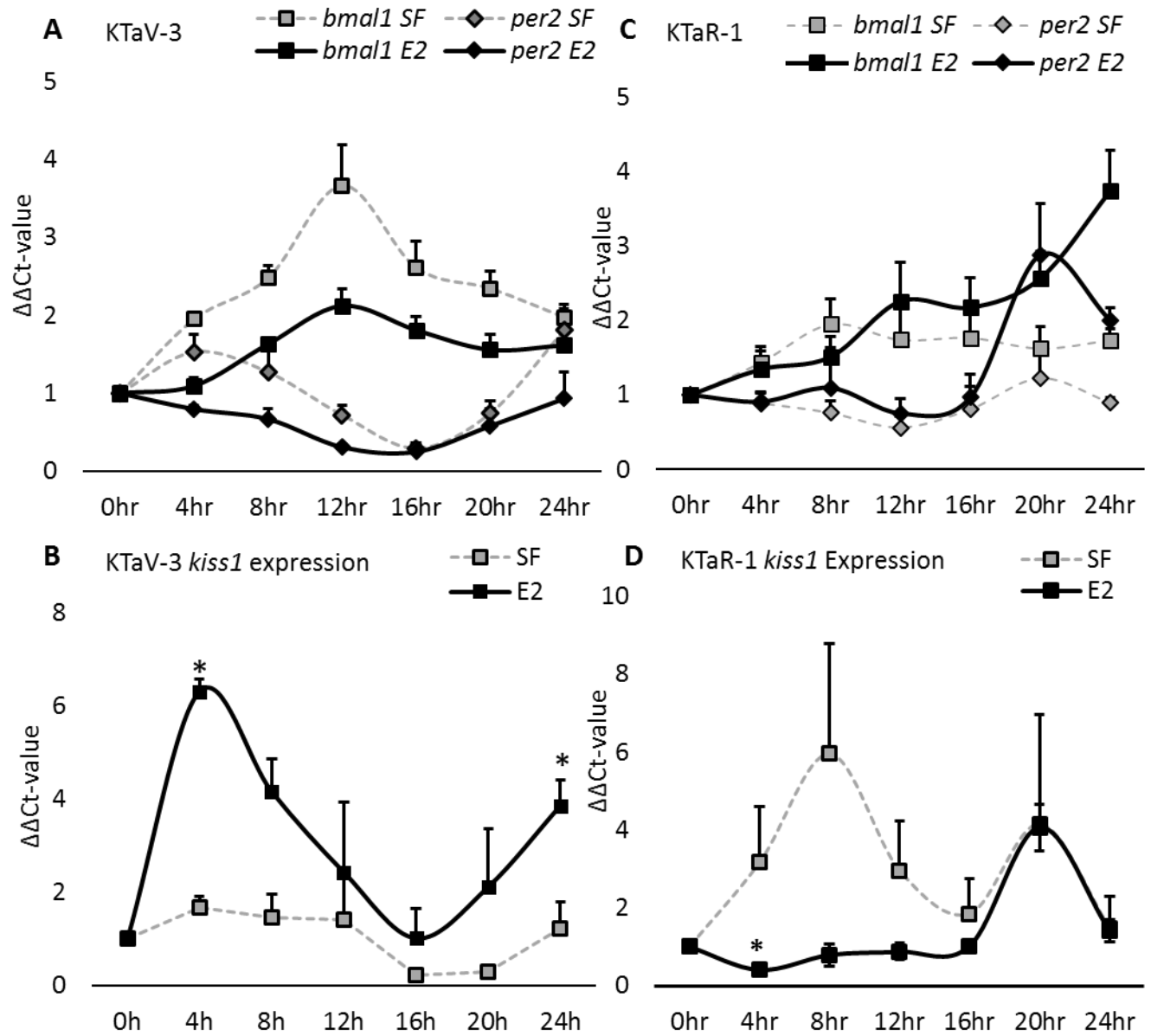


Table 1. Nucleotide sequences of the specific primers used in PCR

Gene	Primer Sequence 5' – 3'	Product Size
<i>kiss1</i>	F: GCTCTGGTGAAGTACGAACTCTGA R: GACACAGAGGAGAAGCAGCA	150 bp
<i>pdyn</i>	F: AGCAGTAAGCAGGTCATTCATCC R: CACGCCATTCTGACTCACTTGT	97 bp
<i>tac2</i>	F: ATCCAACGCTCTTGAGATCA R: CATCTTACCTTACTGAGCCTCC	256 bp
<i>gfap</i>	F: TCCTGGAACAGCAAAACAAG R: CAGCCTCAGGTTGGTTTCAT	224 bp
<i>ppia</i> ¹	F: AAGTTCCAAAGACAGCAGAAAAC R: CTCAAATTTCTCTCCGTAGATGG	100 bp

¹PPIA was used as a housekeeping gene to access quality of cDNA and provide standard for qPCR

Figure Legends

Figure 1. KTaV-3 and KTaR-1 possess a neuronal phenotype (**A** and **C**). **B**, *kiss1*-GFP expression in KTaV-3 and KTaR-1 neurons after FACS (**B** and **D**). **E**, *gfap* expression is not found in KTaV-3 and KTaR-1. “MB” = mouse brain. Both cell types also express *kiss1* (**F**). KTaR-1 cells express significantly higher levels of *tac2* (**G**) and *pdyn* (**H**). **I**, Quantification of the basal expression of *kiss1* between KTaV-3 and KTaR-1 (One-way ANOVA n=3). **J**, Quantification of the basal expression of *esr1/esr2* between cell lines compared to KTaV-3 (^a two sided p-value < 0.05; One-way ANOVA n=4) Data are presented as mean ± SEM.

Figure 2. **A**, Expression changes of *kiss1* at 0 hr, 4 hr, and 24 hr time points in serum free (SF) media with either PBS vehicle or 25 pM E₂ in KTaV-3 (* two-sided p-value < 0.05; One-Way ANOVA n=6). **B**, Expression changes of *kiss1* at 0 hr, 4 hr, 24 hr time points in SF media with either PBS vehicle or 5 pM E₂ in KTaR-1 (* two-sided p-value < 0.005; One-way ANOVA n=4). **C**, Kisspeptin ELISA results from static cells in 10% DMEM FBS maintenance conditions (One-way ANOVA n=3). **D**, Kisspeptin ELISA results (pg/mL) basally (0 h) and after 12 hr exposure to 25 pM E₂ (^a two-sided p-value < 0.001; One-way ANOVA n=3). Data are presented as means ± SEM

Figure 3. *kiss1* expression levels observed in KTaV-3 and KTaR-1 lines after 4 hr exposure to estradiol. *two sided p-value < 0.01; One way ANOVA, n=4. **two sided p-value < 0.01; One way ANOVA, n = 4. Data are presented at means ± SEM

Figure 4. Temporal expression patterns of *bmal1*, *per2*, and *kiss1* for KTaR-1 and KTaV-3. **A**, Expression of *bmal1* and *per2* over 24 hr exposed to PBS vehicle or 25 pM E₂ in KTaV-3. **B**, Expression of *kiss1* over 24 hr with 25 pM E₂ or vehicle in KTaV-3. (*two sided p-value < 0.05; One-way ANOVA, n = 3) **C**, Expression of *bmal1* and *per2* over 24 hr exposed to PBS vehicle or

5pM E₂ in KTaR-1. D, Expression of *kiss1* over 24 hr with 5pM estradiol or vehicle in KTaR-1.

(*two sided p-value < 0.005; One-way ANOVA, n = 4). Data are presented as means ± SEM.

Chapter Two: Divergent roles of ER α and ER β in immortalized AVPV and arcuate neurons

Introduction

Complete maturation of the reproductive axis is contingent on appropriately timed reactivation of quiescent hypothalamic gonadotropin-releasing hormone (GnRH) neurons. Successful progression and termination of puberty culminates in the production of mature gametes and introduction of reproductive activity. This process is not completely understood, though high-frequency GnRH pulses that direct pituitary gonadotropic hormone secretions to mature the hypothalamic pituitary gonadal (HPG) axis, represent the beginning of the transition state between juvenile and adult periods. Factors that govern the onset, progression, and completion of this ill-defined process involve somatic and environmental signals to permit pubertal acceleration resulting in GnRH release. The cellular signaling pathways responsible for activating GnRH neuron activity have yet to be elucidated.

The mechanism for the onset of puberty has been explained in part with the “gonadostat” hypothesis, which states that in prepubertal female mammals, the immature ovary secretes small amounts of estradiol, sufficient to exert negative feedback on the hypothalamus and pituitary to inhibit GnRH and subsequent LH release [97]. However, at the onset of puberty, estradiol levels rise to a critical point to convey positive feedback, thereby eliciting pulses in GnRH to drive the maturation of the reproductive axis. Specific neuronal populations which respond to these differential levels of estradiol via estrogen receptors may mediate the negative to positive feedback transition to achieve the obligatory GnRH pulse profile required to initiate puberty.

The G-protein coupled receptor, KISS1R (also called GPR54) and its cognate ligand, kisspeptin, play an insurmountable role in regulating the HPG axis and orchestrating the timing of

puberty. Inactivating mutations in human *gpr54* have been associated with hypogonadotropic hypogonadism and failure to initiate puberty. Furthermore, ablation of *gpr54* or *kiss1* in mice yield either sex hypogonadotropic and infertile. Kisspeptin neuron involvement in activating GnRH neurons via perikaryon and axon colocalized GPR54 has been corroborated as a potent GnRH secretagogue from kisspeptin administration advancing pubertal onset, whereas GPR54 antagonists delay pubertal onset. Estrogens provide differential regulation of kisspeptin secretion in sexually dimorphic arcuate and anteroventral periventricular (AVPV) nuclei in female rodents. In AVPV nuclei, estradiol provides positive feedback to increase kisspeptin secretions while contemporaneously providing negative feedback to reduce kisspeptin secretions from arcuate nuclei. Estrogen nuclear receptor α (ER α) has been shown to be coexpressed in both AVPV and arcuate hypothalamic nuclei, providing a platform that implicates this receptor as regulating kisspeptin secretions and subsequently directly modulating the timing of puberty. Conditional knockouts of the ER α gene (*esr1*) in kisspeptin neurons results in advancement of pubertal onset in female mouse models. Secondly, complete maturation of the reproductive axis is arrested as typical ovulatory cyclicity is not achieved. However, the transcriptional role of ER α in impacting *kiss1* expression in AVPV and arcuate nuclei independently has not been assessed, mainly due to the innate challenge of implicating specific hypothalamic nuclei roles via *in vivo* models. Therefore, to elucidate the role of estrogen receptors in kisspeptin release we generated immortalized AVPV and arcuate cell models and assessed temporal regulation of *esr1* and *esr2* in these respective hypothalamic lines independently.

Results

*KTaV-3 and KTaR-1 cells basally co-express *esr1* and *esr2**

Standard PCR reveals coexpression of both ER α and ER β genes, *esr1* and *esr2* respectively in both KTaV-3 and KTaR-1 neuronal cell lines maintained in 10% FBS DMEM (**Figure 1**). Basal expression of *esr1* is higher in KTaR-1 relative to KTaV-3 whereas roughly tantamount expression of *esr2* is observable between the two different cell models under the same maintenance conditions.

*Expression of both *esr1* and *esr2* does not change as a function of estradiol dose*

To determine the impact of 17 β -estradiol dose on *esr1* and *esr2* expression, 3cm plates of cells were treated with estradiol doses ranging from 5.0-100.0 pM. RNA was collected in TRIzol, isolated, and analyzed for changes in *esr1* and *esr2* expression. Across all doses, *esr1* and *esr2* expression did not change between both cell types.

*Regulation of *esr1* and *esr2* is unique between KTaV-3 and KTaR-1 treatment conditions*

To determine the overlap between *esr1* and *esr2* expression between both cell types with their concurrent expression differences in *kiss1* shown previously, *esr1* and *esr2* expression changes were evaluated with qPCR following estradiol treatment with serum synchronized cells. In KTaV-3 cells, *esr1* expression was significantly repressed after a 4h exposure to 25.0 pM E2 (0.634 ± 0.049 ; p-value < 0.05), whereas a significant increase in *esr1* expression was observed in control PBS conditions after 24h exposure (3.86 ± 0.964 ; p-value < 0.05) (**Figure 3A**). While not statistically significant, an increase in *esr1* was contemporaneously observed after 24h exposure to 25.0 pM E2 in KTaV-3 cells (8.46 ± 3.37 ; p-value = 0.059) (**Figure 3A**). Expression of *esr2* did

not mirror *esr1* expression in KTaV-3 cells, indeed no statistically significant change was observed for either treatment condition after 4h exposure (**Figure 3B**). However, significant repression of *esr2* was found after 24h exposure to both PBS and 25.0 pM E2 (0.372 ± 0.127 ; p-value < 0.05 and 0.501 ± 0.119 ; p-value < 0.05, respectively) (**Figure 3B**). In KTaR-1 cells, *esr1* expression was not significantly modulated over 4h and 24h time points in 5.0 pM E2 or PBS, though an increasing trend was observed after 24h in both PBS and E2 treatment conditions (3.41 ± 0.777 ; p-value = 0.126 and 7.75 ± 1.65 ; p-value = 0.079, respectively) (**Figure 3C**). Furthermore, *esr2* expression in KTaR-1 cells was significantly repressed after 4h exposure to PBS (0.703 ± 0.062 ; p-value < 0.05) and 5.0 pM E2 (0.599 ± 0.003 ; p-value << 0.001) (**Figure 3D**). Finally, after 24h exposure to 5.0 pM E2, *esr2* expression increased significantly (2.52 ± 0.356 ; p-value < 0.05) (**Figure 3D**).

Estradiol differentially regulates temporal esr1 and esr2 expression in KTaV-3 and KTaR-1 cells

To explore temporal changes in *esr1* and *esr2* expression in these two cell types following estradiol exposure, we converted RNA to cDNA from samples harvested every 4 hours for 24 hours following either vehicle (PBS) or 17β -estradiol treatment, and examined expression profiles of core circadian clock genes. As outlined previously, 25.0 pM and 5.0 pM E2 were used for KTaV-3 and KTaR-1 cell, respectively for this investigation. In KTaV-3 cells, *esr1* expression increased significantly relative to 0h at 8h, 12h, and 16h only with PBS (2.05 ± 0.218 ; p-value < 0.05, 1.69 ± 0.098 ; p-value < 0.05, and 2.89 ± 0.431 ; p-value < 0.05, respectively) (**Figure 4A**). No significant increases in *esr1* expression was observed for KTaV-3 cells under estradiol treatment conditions at these particular time points (**Figure 4A**). However, *esr2* expression was divergently regulated in KTaV-3 cells, with significant repression of this gene observed at the 16h and 20h

time points in control conditions (0.458 ± 0.172 ; p-value < 0.05 and 0.313 ± 0.106 ; p-value < 0.05 , respectively) (**Figure 4B**). Furthermore, *esr2* expression was also suppressed at the 20h time point in KTaV-3 cells with 25.0 pM E2 (0.453 ± 0.201 , p-value < 0.05) (**Figure 4B**). For KTaR-1 cells, a statistically significant change in *esr1* expression was only observed after 12h exposure to control PBS conditions (1.74 ± 0.112 ; p-value < 0.05) (**Figure 4C**), though an insignificant upward trend of *esr1* was also noted at further time points, beginning at 20h. Finally, *esr2* expression in KTaR-1 is repressed at 12h and 16h under PBS conditions (0.499 ± 0.066 ; p-value < 0.05 and 0.531 ± 0.091 ; p-value < 0.05 , respectively) (**Figure 4D**). This repression was not mirrored in 5.0 pM E2 conditions, though the apparent increased expression levels of *esr2* in estradiol treatment conditions was not statistically significant (**Figure 4D**).

Discussion

This is the first study to use immortalized AVPV and arcuate neurons from a fully differentiated adult female mouse to investigate the expression patterns of *esr1* and *esr2* to identify their roles in each nucleus independently. By using immortalized neurons from this well-defined murine model, a high resolution investigation of the role of these nuclear estrogen receptors can be achieved. Here, we implicate the role of 17β -estradiol in modulating the expression levels of *esr1* and *esr2* in these recently generated neuronal models.

Validation of esr1 and esr2 expression in immortalized neurons

Immortalized KTaV-3 and KTaR-1 cells co-express *esr1* and *esr2* in basal conditions, implicating their capacity to respond to 17β -estradiol. From the previous work, basal levels of *esr1* appear to be higher in KTaR-1 neurons whereas *esr2* expression are roughly equal. Furthermore,

basal levels of *esr1* and *esr2* expression do not change as a function of estradiol dose. From the diestrus level of estradiol (5.0 pM E2) to the super-physiological level (100 pM E2), abundance of *esr1* and *esr2* do not significantly change across the entirety of the dose range. This suggests that in both AVPV and arcuate models that expression modulation of these ER α and ER β nuclear receptor genes does not change with rising or falling concentrations of estradiol, rather expression remains relatively consistent. However, to conclude whether or not this translates to ER α / β abundance fluctuation in cytosolic environments will require further investigation.

*Exploring estradiol modulation of temporal *esr1* and *esr2* expression patterns*

While several *in vivo* studies have implicated the role of estrogen nuclear receptors, particularly ER α , in hypothalamic AVPV and arcuate nuclei, few have investigated the temporal expression patterns and role of estradiol for *esr1* and *esr2* in these neurons independently. Whereas estradiol dose has little to no effect on *esr1* or *esr2* expression in either neuronal model, expression differences are measurable as a function of time with serum synchronized conditions, but not necessarily unique from control conditions. In KTaV-3 cells, *esr1* expression is initially repressed by 25.0 pM E2 that is not seen in the control condition whereas *esr2* expression remain consistently similar to basal 0h levels until 20h under the same 25.0 pM E2 treatment condition. This repression of *esr2* expression is propagated until 24h with 25.0 pM E2, however cotemporaneous increased expression of *esr1* is initiated (though not significantly) at 16h that is sustained until 24h, though this increased expression of *esr1* is in both treatment conditions for KTaV-3 cells. Interestingly, expression of *esr1* and *esr2* is not significantly modulated by estradiol in KTaV-3 cells, though the rise of *esr1* expression at 16h that is propagated by estradiol and simultaneously met with decreases in *esr2* expression under the same estrogenic treatment at the same time points is

mechanistically intriguing. Together, these data suggest that *esr1* expression in KTaV-3 cells is initially low and estradiol does not necessarily illicit the uniquely divergent expression alteration at further time points in these neuronal models. This rise in *esr1* expression to generate a neuron ostensibly more sensitive to physiological estradiol is not necessarily permitted by rising hormonal levels, rather it may be gated by an intracellular mechanism that remains to be elucidated. With *esr2* expression, the eventual increased expression observed with *esr1* is not mirrored, suggesting that the stimulatory role of AVPV neurons *in vivo* is largely impacted by ER α rather than ER β , or that the positive feedback characteristic unique to these neurons in the context of estrogen signaling may be provided by an overabundance of ER α relative to ER β . As shown previously, in serum synchronized KTaV-3 cells there is a significant increase in *kiss1* transcriptional activity at both 4h and 24h time points in the presence of 25.0 pM estradiol. In the context of this work, it would appear that given the remarkably low abundance of *esr1* transcriptional activity at 4h followed by significantly higher expression of *esr1* at 24h, that these peaks of *kiss1* transcription are mediated by different estrogenic signaling mechanisms. The initial peak of *kiss1* expression may be permitted by a membrane bound estrogen receptor given the low abundance of *esr1* at that point in time. However, the subsequent 24h peak in *kiss1* activity could be achieved by the rising abundance of *esr1*. Therefore, the possibility that the unique peaks in *kiss1* transcriptional activity found in these KTaV-3 cells are regulated by two different estrogen signaling mechanisms, one non-classical and the other classical, has escaped the scope of this investigation and will require further delineation in subsequent publications.

In KTaR-1 cells, *esr1* expression was not significantly modulated by either 5.0 pM estradiol treatment or control for the entirety of the time course, save for an isolated time point. It should be noted that while the increase in *esr1* expression is not statistically significant, the obvious

trend is that in the arcuate model estradiol increases abundance of *esr1* transcript that is more robust compared to control conditions at higher time points. This over expression of *esr1* is simultaneously met with an increased expression of *esr2* after 24h exposure to 5.0 pM estradiol that is not observable in control conditions. Therefore, these data suggest that high co-expression of ER α and ER β genes is present in arcuate model lines that is absent in the AVPV model.

It has been previously shown in human osteoblastic cell lines that coexpression of ER α and ER β reduces the transcriptional capacity of either nuclear receptor alone, thereby providing a mechanism for mutual antagonism when both nuclear receptors are present in a cell [98]. Furthermore, previous work in GT1-7 cells (a GnRH model) has implicated the role of ER α alone as being responsible for increased promoter activity of *kiss1* *in vitro* in the presence of estrogen [99]. Taken together, this report suggests that the divergent regulation of kisspeptin release by estradiol in AVPV and arcuate neurons is due in part by differential expression and abundance of ER α and ER β genes. In AVPV neurons, the positive feedback mechanism for kisspeptin-release unique to this hypothalamic neuronal population is achieved in part by rising transcriptional levels of *esr1* over *esr2*, providing the cell the capacity to activate this estrogen-sensitive gene through a classical genomic signaling pathway without the antagonistic effects of competitory ER β . Alternatively, in arcuate neurons rising levels of ER α coincides with rising abundance of ER β , thereby providing mutual antagonism that prevents the cell from activating estrogen-responsive genes, such as *kiss1*. Future investigations will identify the role of potentially recruited cofactors that have been implicated in regulating the divergent role of estrogen feedback between these hypothalamic subpopulations, as well as the impact of ER α and ER β agonists and antagonists to further elaborate the mechanism behind divergent estrogen signaling in AVPV and arcuate neurons to elucidate their contributions to the mammalian HPG axis.

Figures

Figure 1:

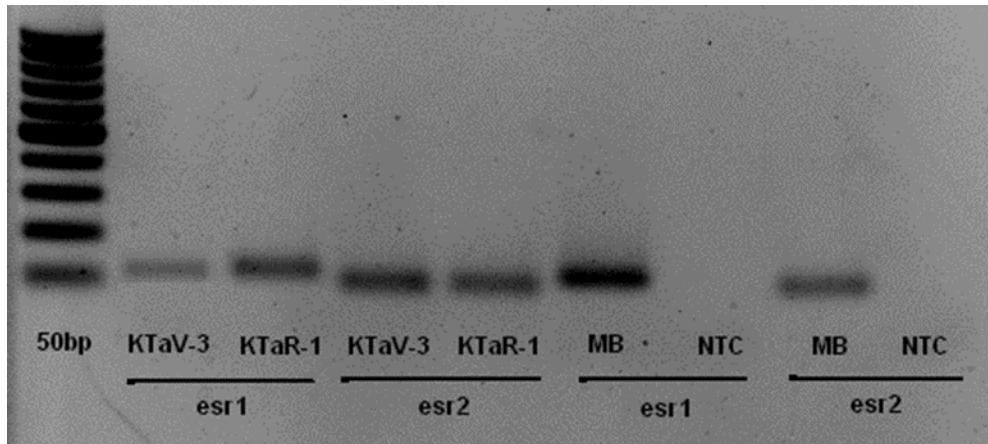


Figure 2:

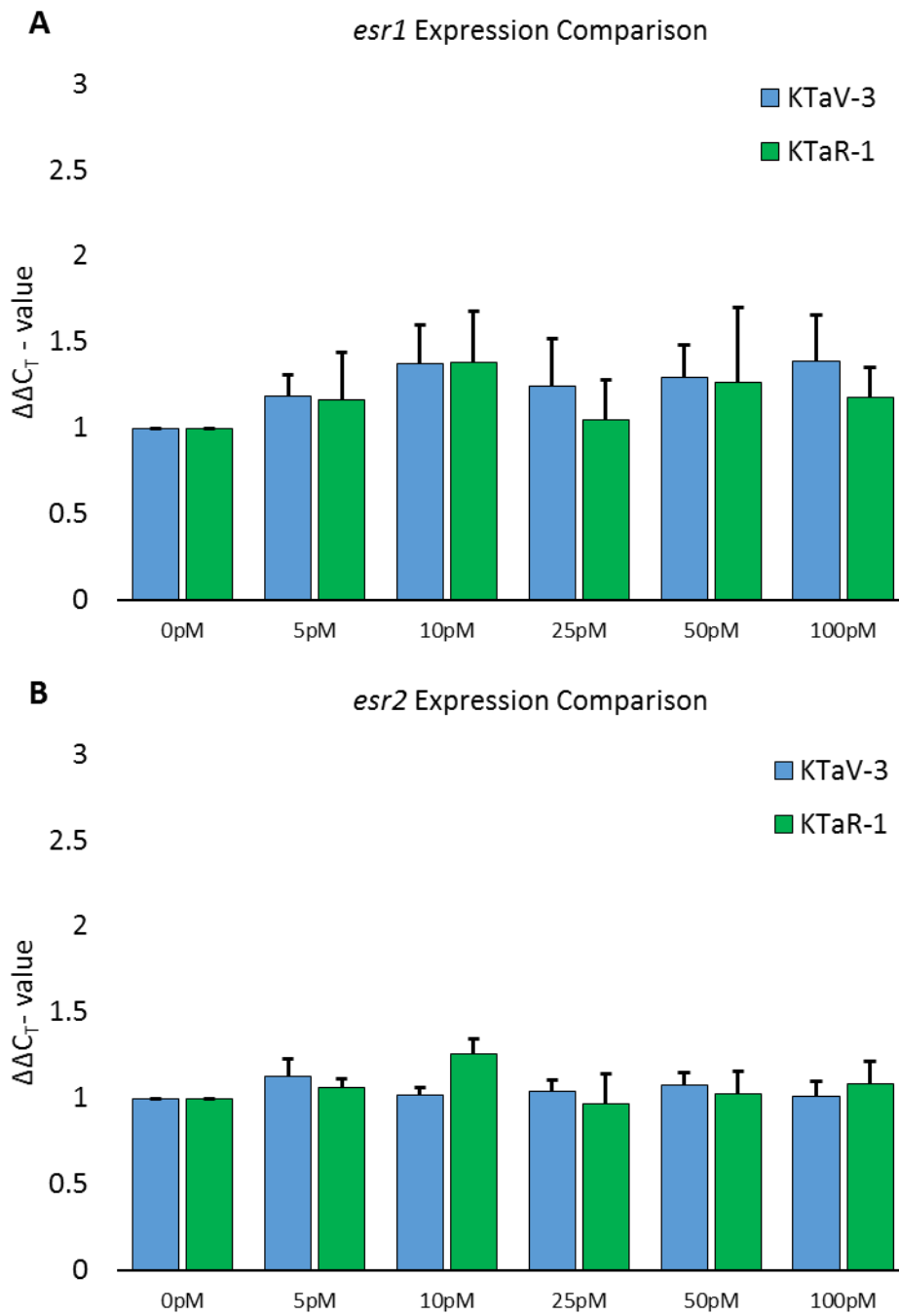


Figure 3:

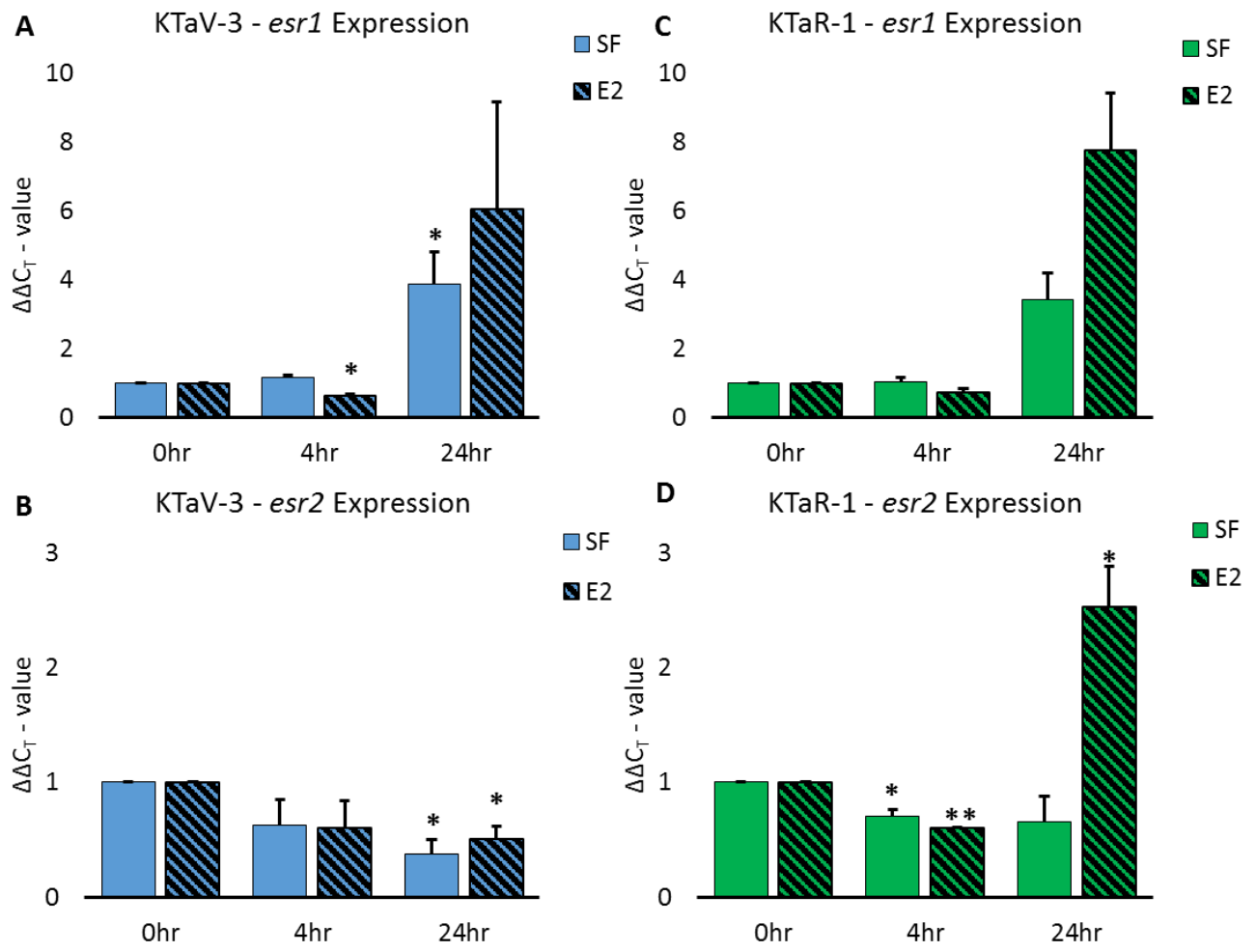


Figure 4:

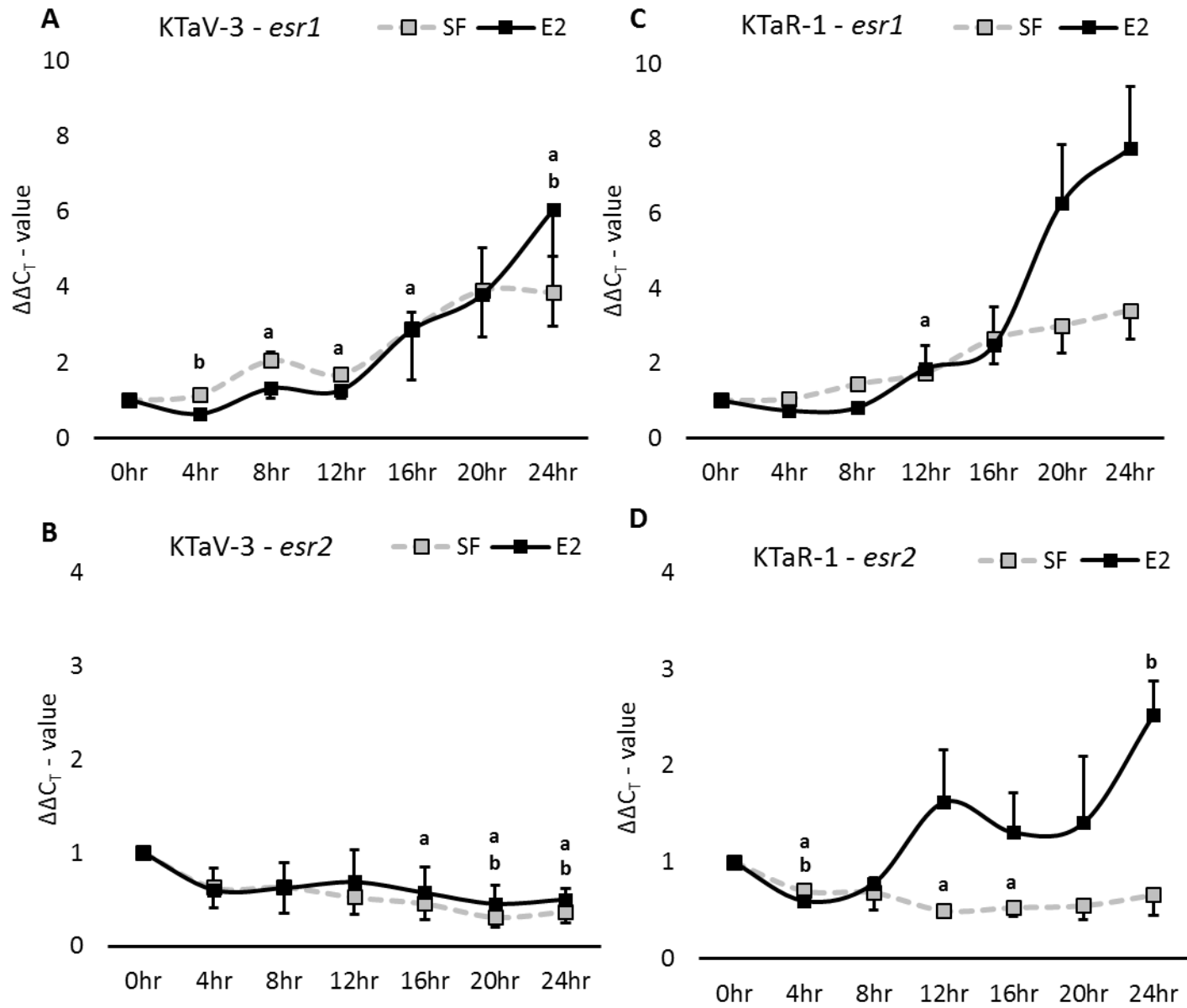


Figure Legends

Figure 1. KTaV-3 and KTaR-1 possess *esr1* and *esr2* transcripts. “MB” = mouse brain.

Figure 2. *esr1* and *esr2* expression levels observed in KTaV-3 and KTaR-1 lines after 4h exposure to estradiol. No statistical significance measured relative to 0hr treatment using One-Way ANOVA (n = 4).

Figure 3. A, Expression changes of *esr1* at 0h, 4h, and 24h time points in serum free (SF) media with either PBS vehicle or 25.0 pM E₂ in serum synchronized KTaV-3 cells (* two-sided p-value < 0.05; One-Way ANOVA n = 3). **B,** Expression changes of *esr2* at 0h, 4h, 24h time points in SF media with either PBS vehicle or 25.0 pM E₂ in KTaV-3 cells (* two-sided p-value < 0.05; One-way ANOVA n = 3). **C,** Expression changes of *esr1* at 0h, 4h, and 24h time points in SF media with either PBS vehicle or 5.0 pM E₂ in KTaR-1 cells (No statistical significance measured using One-Way ANOVA n = 3). **D,** Expression changes of *esr2* at 0h, 4h, and 24h time points in SF media with either PBS vehicle or 5.0 pM E₂ in serum synchronized KTaR-1 cells (* two-sided p-value < 0.05, **two-sided p-value << 0.001; One-Way ANOVA n = 2). Data are presented as means ± SEM and relative to 0h treatment.

Figure 4. Temporal expression patterns of *esr1* and *esr2* for KTaV-3 and KTaR-1. **A,** Expression of *esr1* over 24h exposed to PBS vehicle or 25.0 pM E₂ in KTaV-3 (^a p-value < 0.05 SF, ^b p-value < 0.05 E₂; One-Way ANOVA n = 3). **B,** Expression of *esr2* over 24h with 25.0 pM E₂ or vehicle in KTaV-3 (^a p-value < 0.05 SF, ^b p-value < 0.05 E₂; One-Way ANOVA n = 3) **C,** Expression of *esr1* over 24h exposed to PBS vehicle or 5.0 pM E₂ in KTaR-1 (^a p-value < 0.05 SF; One-Way ANOVA n = 2). **D,** Expression of *esr2* over 24h with 5.0 pM estradiol or vehicle in KTaR-1 (^a p-value < 0.05 SF, ^b p-value < 0.05 E₂; One-Way ANOVA n = 3). Data are presented as means ± SEM and relative to 0h treatment.

Chapter 3: Kiss1 expression is modulated by estrogen and endocrine disruptors in immortalized female AVPV- and arcuate specific neuronal kisspeptin cell lines

Abstract

Ovulation requires preovulatory surges of gonadotropin-releasing hormone (GnRH) from preoptic hypothalamic neurons, initiated by elevated ovarian estradiol (E_2). Rising E_2 activates a subset of sexually dimorphic kisspeptin (Kiss-1) neurons in the female, located in the anteroventral periventricular nuclei (AVPV). Conversely, estradiol negative feedback on GnRH secretion is mediated by a neuroanatomically separate population of Kiss-1 neurons in the arcuate nuclei. Kisspeptin stimulates GnRH expression and secretion *in vivo*, and the development of this system is critical for the initiation of puberty. To elucidate how phenotypically similar Kiss-1 neuronal populations react differentially to E_2 exposure, we have generated two immortalized Kiss-1 cell lines from *kiss1*-GFP post-pubertal female mice. These cell models recapitulate *in vivo* differential responsiveness to E_2 , with KTaV-3 (AVPV-derived) demonstrating ~6-fold increases in *kiss1* expression under higher E_2 doses (5pM – 50pM E_2), while *kiss1* expression in KTaR-1 cells is suppressed up to 80% under lower E_2 concentrations (2pM – 10pM). Further, we have found that baseline expression of estrogen receptor α ($ER\alpha$ /*esr1*) is significantly different between these lines, with KTaR-1 cells exhibiting a 5-fold higher expression of *esr1* relative to KTaV-1, whereas estrogen receptor β ($ER\beta$ /*esr2*) is not differentially expressed. Additionally, we are exploring the impact of endocrine disrupting class of perfluorinated alkyl substances (PFASs) on these neurons, with preliminary results illustrating *kiss1*, *esr1*, and *esr2* transcriptional activation and/or repression at relevant doses of perfluorooctanoic acid, perfluorooctanesulfonic acid, and perfluorohexanoic acid in the two lines. Finally, we are probing temporal patterns of *kiss1* and core

clock gene expression in these lines in response to estradiol, and find distinct antiphasic patterns of *bmal1* and *per2* in KTaV-3 cells irrespective of E₂ exposure. Treatment of KTaV-3 cells with 25pM E₂, however, elicited distinct patterns of *kiss1* expression over time in contrast to vehicle, suggesting differential coupling of intracellular oscillators to *kiss1* transcriptional activity in the presence of E₂. Ongoing delineation of responsiveness to E₂ in these lines could reveal novel molecular mechanisms underlying differential expression patterns demonstrated *in vivo* between these neuronal populations. Furthermore, investigating the impact of select PFASs on transcriptional activity of *kiss1*, *esr1*, and *esr2* between these two cell lines could elucidate the consequence of estrogen mimicry during sex-steroid sensitive developmental phases.

Introduction

Endocrine disrupting compounds (EDCs) have received increasing attention from the scientific community as they may pose a significant threat to human health by interfering with physiological hormone regulation and function. This interference can result in deviation from normal homeostatic control and can reprogram normal developmental and reproductive processes. Many EDCs can impact normal activity of estrogen receptors (ER) as they have estrogen mimetic properties. However, the structural moiety by which several classes of EDCs attain nuclear ER α and ER β ligand affinity is not necessarily consistent, though EDCs that belong to the same group in terms of chemical structure tend to have comparable ER α and ER β estrogen-response-element mediated activities. Estrogens play an essential role in the moderating the mammalian reproductive axis by allowing both positive and negative feedback regulation through two hypothalamic subpopulations, the anteroventral periventricular (AVPV) and arcuate nuclei, respectively. These

subpopulations release kisspeptin, encoded by *kiss1*, to drive the onset of puberty and are considered absolutely essential in maintaining appropriate functioning of the reproductive axis.

A class of EDCs that are considered to have estrogen mimetic properties are perfluorinated alkyl substances (PFASs). PFASs are found in food packaging, firefighting foam, cosmetics and insecticides; dietary intake is considered the most critical route of exposure. Perfluorooctanoic acid (PFOA) and perfluorooctane sulfonate (PFOS) are the most prevalent PFASs found in human serum. PFOS and PFOA have also been detected in several human tissues including umbilical cord blood, breast milk, and nervous tissue, attached to proteins rather than lipids. Considering that PFASs are capable of traversing the placental barrier, the developing fetus is exposed to these chemicals at an incredibly sensitive window of development. Recently, PFASs have been implicated in reducing human fertility: higher PFOS and PFOA levels have been associated with longer time to pregnancy and irregular menstrual cycles. Men with higher PFOS and PFOA concentrations in serum had severely reduced sperm counts compared to men with lower PFAS abundance. Animal studies have provided a platform to elucidate mechanisms of action by which PFASs impact human health, though the exposure levels used in these studies do not recapitulate relevant environmental exposures measured in humans. Furthermore, to identify the potency of particular PFASs in specific target tissues, it is fortuitous to use an *in vitro* model where dose and exposure can be robustly controlled, and absorption, distribution, metabolism, and excretion factors associated with an *in vivo* approach can be avoided

Therefore to assist in the understanding of how PFASs impact cellular functioning and the impact of estrogen mimicry for three PFASs: PFOS, PFOA, and perfluorohexanoic acid (PFHxA), we have used two immortalized neuronal cell lines that are accurate models for AVPV and arcuate

subpopulations. Using these lines, we can identify high resolution transcriptional modulation of target genes post environmentally relevant exposure to PFOS, PFOA, and PFHxA compounds.

Results

Transcriptional modulation of kiss1, esr1, and esr2 target genes following PFAS exposure

To determine the influence of PFOS, PFOA, and PFHxA on *kiss1*, *esr1*, and *esr2* expression, we performed a dose response analysis with fM, pM, and nM levels of each corresponding PFAS with DMSO control. For *kiss1* expression, 25.0 fM PFOS elicited an 8-fold increase in transcriptional activity in KTaR-1 cells (8.35 ± 2.93 ; p-value < 0.05), whereas 25.0 nM PFOS provoked a repression of *kiss1* in KTaR-1 cells (0.502 ± 0.161 ; p-value < 0.05) (**Figure 1A**). KTaV-3 cells did not have any statistically significant change in *kiss1* expression over the entire dose range for PFOS. However, PFOA did increase expression of *kiss1* in KTaV-3 cells at a 25.0 fM concentration (7.12 ± 0.643 ; p-value < 0.05) (**Figure 1B**). In KTaR-1 cells, *kiss1* was repressed at the same concentration (0.602 ± 0.107 ; p-value < 0.05) (**Figure 1B**). When exposed to 25 fM PFHxA, *kiss1* expression was sufficiently modulated in KTaR-1 cell alone (2.41 ± 1.06 ; p-value < 0.05) (**Figure 1C**). KTaV-3 cells were not significantly altered in terms of *kiss1* transcriptional activity when exposed to PFHxA (**Figure 1C**). PFOS, PFOA, and PFHxA did not have any appreciable influence on *esr1* expression in either cell type across the entirety of the dose response (**Figure 2A, 2B, 2C**, respectively). PFOS, PFOA, and PFHxA also had no effect on *esr2* expression in either cell type (**Figure 3A, 3B, 3C**, respectively).

Discussion

This is the first study to implicate the influence of a group of common PFASs on *kiss1*, *esr1*, and *esr2* expression in immortalized AVPV and arcuate models to take a necessary step to delineate the mechanism of action by which these EDCs impact the mammalian reproductive axis. This is among the first studies to use extremely low doses of PFOS, PFOA, and PFHxA to illicit a transcriptional response via an *in vitro* model and will prove as a valuable platform for future investigations to elucidate the molecular mechanism responsible for the transcriptional modulation described here. An inherent limitation associated with this study is the dependence on an *in vitro* cell model to use as a proxy for two hypothalamic neuronal populations sensitive to estrogenic signaling. The exposure profile presented here is not necessarily recapitulative of the more relevant chronic exposure to these chemicals that occurs over a lifetime. In addition, this study uses single dose PFOS, PFOA, or PFHxA; therefore the impact of complex mixtures demonstrated in environmental compartments cannot be ascertained.

One of the most significant findings to our study is that fM concentrations of PFOS, PFOA, or PFHxA provoke a remarkable response from AVPV and arcuate neurons in a divergent manner. The current paradigm associated with AVPV and arcuate nuclei in regards to estrogen feedback is that *kiss1* expression is stimulated in AVPV subpopulations whereas a repression occurs in arcuate subpopulations. Therefore, adhering to this paradigm, *kiss1* expression would be stimulated in AVPV, whereas the opposite would be expected from arcuate nuclei. From this study, it becomes clear that depending on the particular estrogenic PFAS (and dose), typical stimulation of *kiss1* or repression of *kiss1* is not necessarily recapitulated. PFOS caused a remarkable increase in *kiss1* expression in arcuate models whereas no effect was observed in the AVPV models. However, at higher doses of PFOS, expected repression of *kiss1* was observed in the arcuate models.

Furthermore, PFOA caused a more estrogenic response in KTaV-3 and KTaR-1 lines that is congruent with the current paradigm associated with this hypothalamic neuronal populations: PFOA caused an increase in kiss1 expression in KTaV-3 lines but a repression in KTaR-1, both at an extremely low dose of this particular EDC. Taken together, these data suggest that different members of PFAS family have unique estrogenic properties that is dependent on the hypothalamic population being exposed. Considering the likeness to physiological 17β -estradiol that PFOA presents at this extremely low dose, exposure to this PFAS may inappropriately activate the HPG axis during a developmental state when the rest of the endocrine system cannot provide the necessary coordinated effort gated by typical estrogenic signaling to initiate pubertal onset. Furthermore, PFOS may be a potent activator of kiss1 expression in arcuate neurons, which would forfeit the negative feedback of endogenous estrogen. Much like what has been shown previously with estradiol having little impact on inducing *esr1* and *esr2* gene transcription, these PFASs likewise do not have an appreciable effect on transcriptional activity of these target genes.

It should be noted that these transcriptional modulation events are only measurable at extremely low doses of PFOS, PFOA, and PFHxA, and these expression differences are not observed at pM and nM levels for the most part. Thusly, it would appear that there is an unidentified compensatory mechanism at play that prevent transcriptional modulation at these higher doses. It is possible that physiological 17β -estradiol, present at pM levels, has a higher affinity for ER α and ER β than PFOS, PFOA, and PFHxA when these substances are presented at pM and nM levels. Future investigations will focus on identifying the mechanism by which these PFASs divergently upregulate kiss1 activity in these immortalized AVPV and arcuate models.

Acknowledgements

We would like to thank Dr. Jennifer Field for her donation of the PFOS, PFOA, and PFHxA standards for use in this work.

Figures

Figure 1:

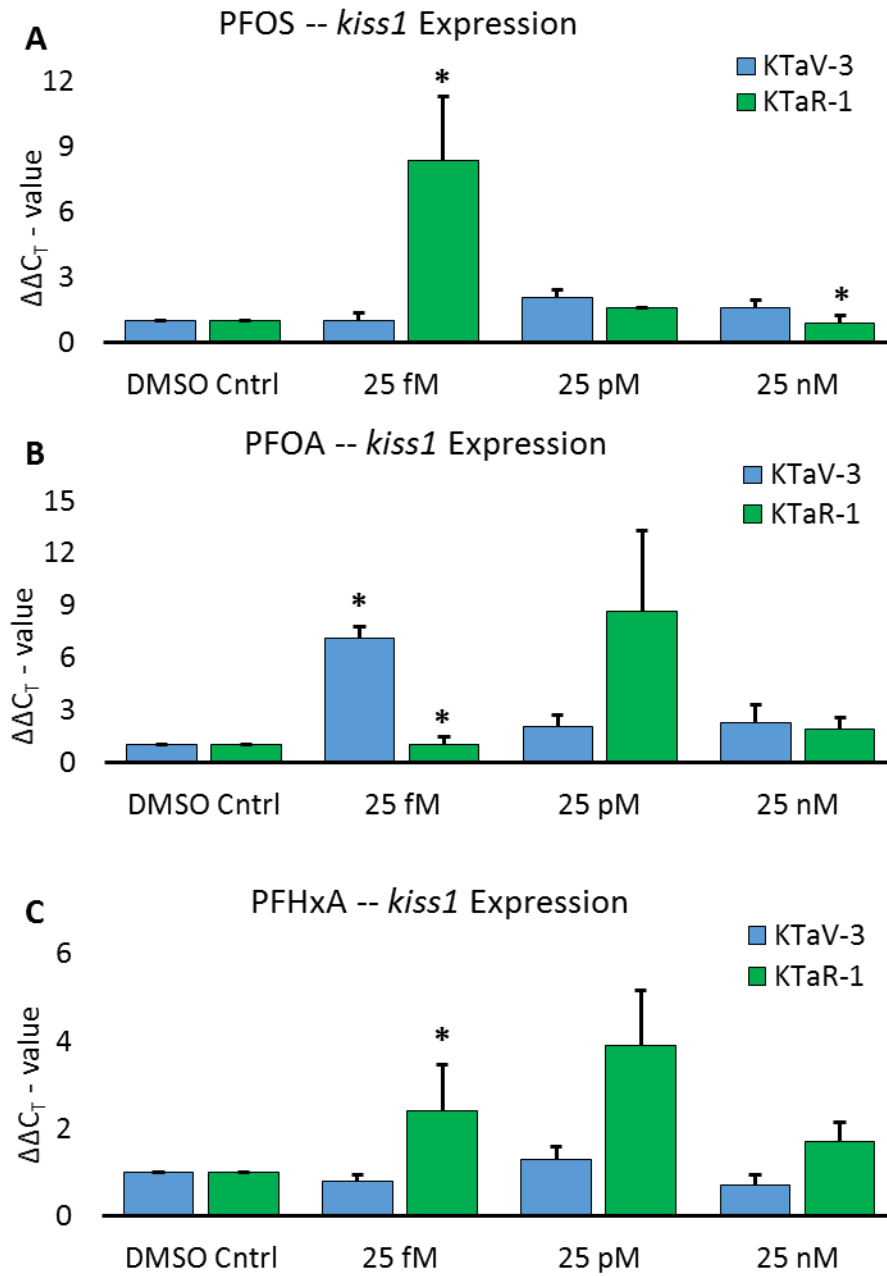


Figure 2:

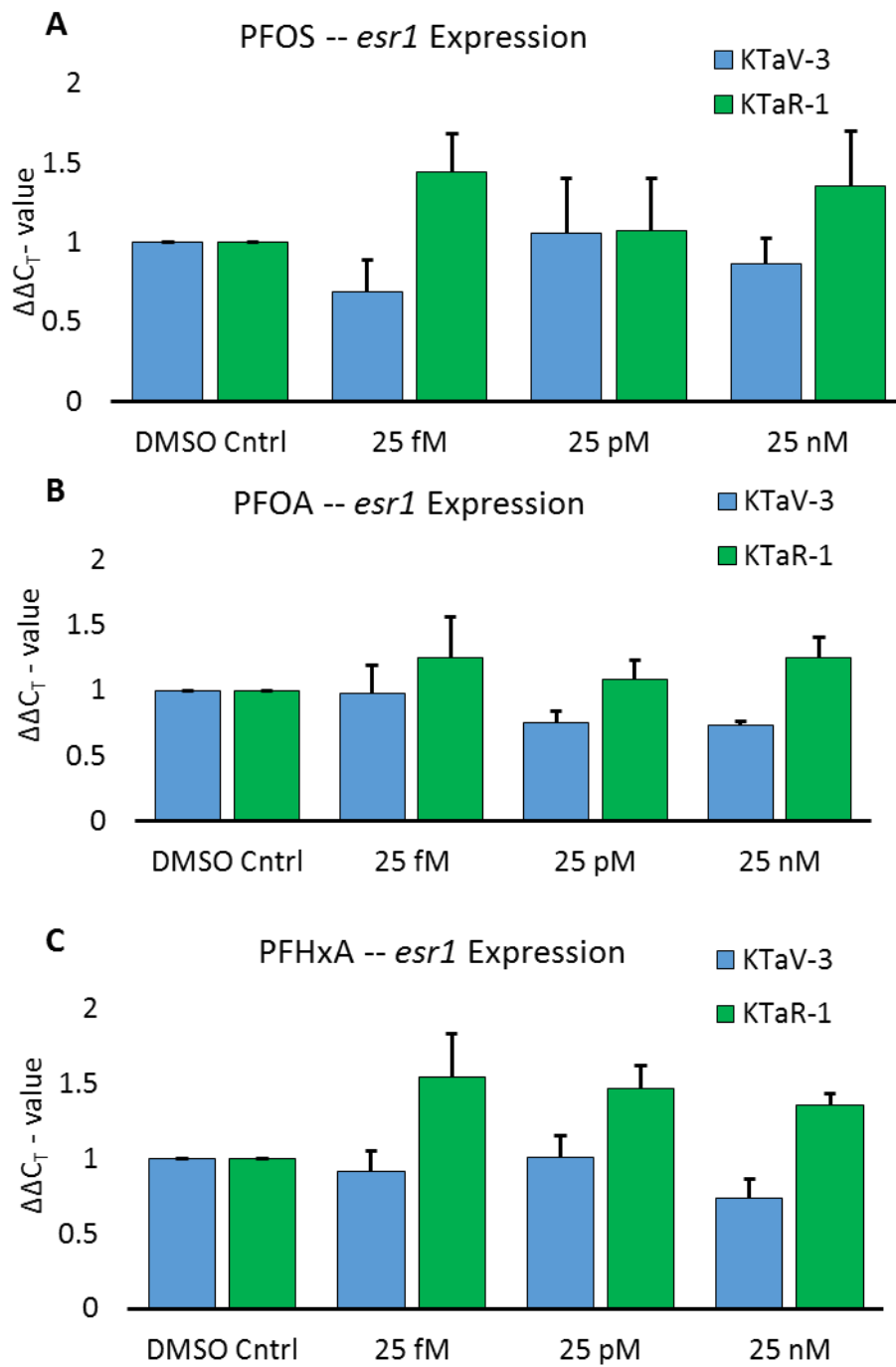


Figure 3:

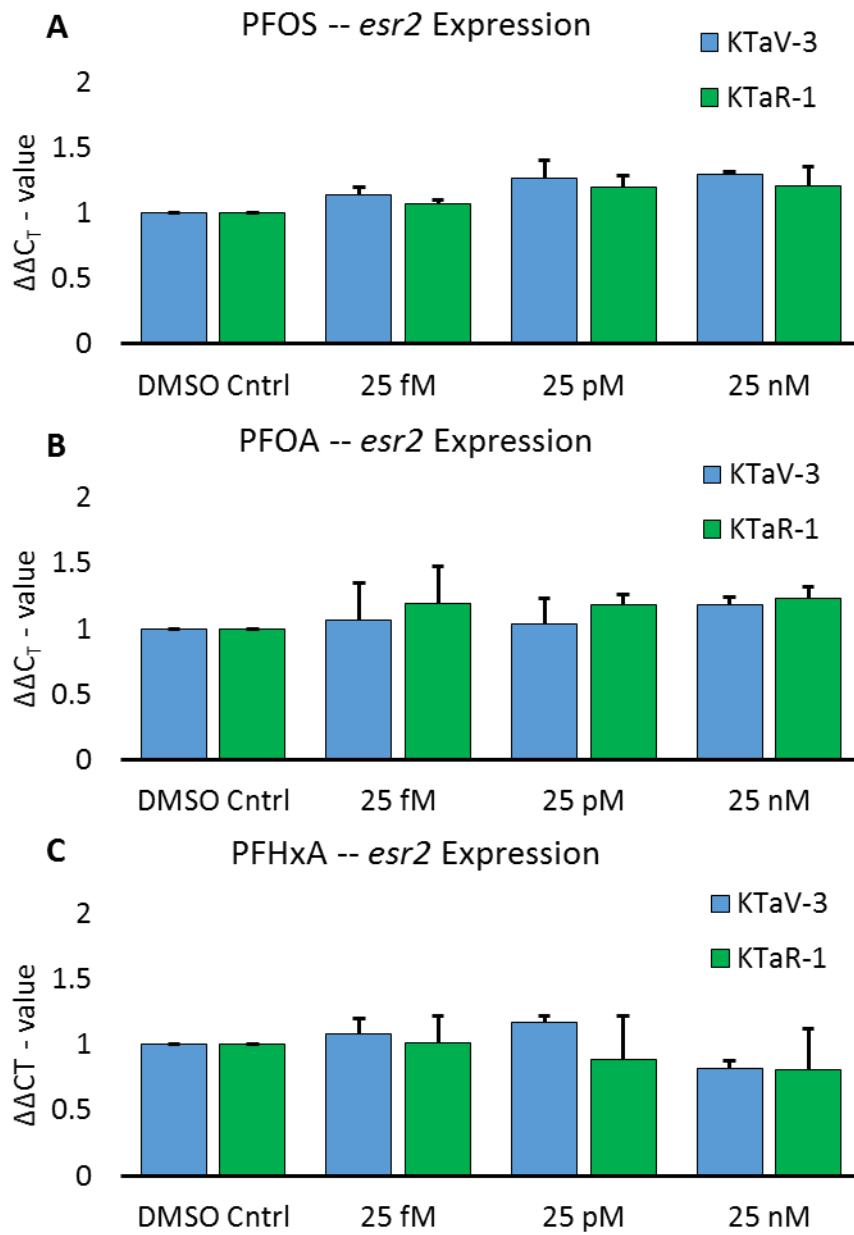


Figure Legends

Figure 1. Dose response impact on kiss1 exposure post 4h exposure to 25 fM, 25 pM, and 25 nM PFOS/PFOA/PFHxA. **A**, Expression modulation of kiss1 after 4h exposure to 25 fM, 25 pM, and 25 nM PFOS (* two sided p-value < 0.05, One-Way ANOVA n=5). **B**, Expression modulation of kiss1 after 4h exposure to 25 fM, 25 pM, and 25 nM PFOA (* two sided p-value < 0.05, One-Way ANOVA n=5). **C**, Expression modulation of kiss1 after 4h exposure to 25 fM, 25 pM, and 25 nM PFHxA (* two sided p-value < 0.05, One-Way ANOVA n=5). Statistical analysis performed relative to DMSO control.

Figure 2. Dose response impact on esr1 exposure post 4h exposure to 25 fM, 25 pM, and 25 nM PFOS/PFOA/PFHxA. No statistically significant change.

Figure 3. Dose response impact on esr2 exposure post 4h exposure to 25 fM, 25 pM, and 25 nM PFOS/PFOA/PFHxA. No statistically significant change.

Final Discussion

Here we described two neuronal cell models that are accurate depictions of female mouse AVPV and arcuate hypothalamic subpopulations: KTaV-3 and KTaR-1, respectively. These cells demonstrate a homogenous neuronal phenotype and do not express glial specific genes. We have used these cells to understand the temporal expression patterns of both ER α and ER β genes to explore the role of each nuclear receptor independently in determining *kiss1* transcriptional activity in both cell types. Furthermore, given their accuracy in being recapitulative models of AVPV and arcuate neurons, we have used these cells as a platform for toxicological studies regarding PFASs and their impact on the HPG axis via these neuronal subpopulations.

KTaV-3 and KTaR-1 neurons demonstrate the *in vivo* observation of differential *kiss1* transcriptional response to endogenous estradiol signaling. KTaV-3 cells increase both transcription and secretion of *kiss1* and the neuropeptide at physiologically relevant levels of estradiol. We have demonstrated that this upregulation of *kiss1* activity as a function of estradiol exposure results in a concurrent increase in kisspeptin secretion in KTaV-3 cells, whereas the downregulation of *kiss1* activity under the same conditions in KTaR-1 cells results in a reduced kisspeptin secretion. This is the first data to demonstrate this phenomena, as the paradigm associated with AVPV and arcuate differential *kiss1* regulation has been observed transcriptionally, not translationally due to the limitation of *in vivo* approaches and reliance on *in situ* hybridization. These data fortifies the prospective utility in using these cells to explore secretion dynamics of these particular hypothalamic subpopulations *ex vivo*. We have also been able to explore the temporal dynamics of *kiss1* expression and circadian core oscillator genes *bmal* and *per2*.

Interestingly, in KTaV-3 cells, there are two repeating peaks of *kiss1* transcriptional activation that are estradiol mediated at 4hr and 24hr whereas without estradiol *kiss1* expression is constitutively low. Furthermore, the overlapped transcription activity of *esr1* and *esr2* did not necessarily overlap with these repeating peaks. Indeed, both *esr1* and *esr2* are not highly expressed at the 4hr peak of *kiss1* expression under estradiol conditions. However, regardless of treatment condition, *esr1* expression steadily increases over time, whereas *esr2* expression remains constitutively low. This data implicates the role of ER α as having a more dynamic role in *kiss1* transcriptional activation in KTaV-3 cells relative to ER β . In addition to this conclusion, the repeating peaks of *kiss1* upregulation in KTaV-3 cells may be mediated by a non-classical estrogen signaling cascade initially at 4h followed by a classical estrogen signaling mechanism at 24h that is dependent on ER α and not ER β . Lastly, the temporal expression of core clock genes *bmal* and *per2* demonstrate the expected antiphasic relationship expected in cells with a functional endogenous clock, though the phase and amplitude is unaffected by estradiol. This suggests that these recurring peaks in *kiss1* expression are not only coupled to the endogenous clock, but is also gated by estradiol.

In KTaR-1 cells, *kiss1* expression is robustly repressed by estradiol at 4h and remains constitutively low until 20h, where a peak in *kiss1* is observed, followed by a return to baseline expression levels. Prior to this experimentation, these cells are maintained in estradiol-containing FBS, therefore the relief of repression observed at 8h without serum demonstrates these cells remarkable sensitivity to estradiol. We have also demonstrated that the temporal expression of *esr1* and *esr2* in KTaR-1 cells is unique from KTaV-3 cells, offering a potential mechanism by which differential regulation of *kiss1* transcription is regulated between these two cell types. Much like KTaV-3 cells, *esr1* and *esr2* expression is initially low in KTaR-1 cells, however tandem

transcriptional activation of both these genes occurs steadily beyond this point in time. *Esr1* expression is driven upwards regardless of treatment in KTaR-1, however, *esr2* is upregulated only in the presence of estradiol. Therefore, after 24h, there is an abundance of *esr1* and *esr2* transcript in KTaR-1 cells only under estradiol conditions that is not observed in KTaV-3 neurons. Therefore, the near constitutive repression of *kiss1* observed beyond the initial 4h time point in KTaR-1 cells may be a function of overabundant ER α and ER β nuclear receptors that bar *kiss1* promoter activation.

Finally, we have used these cell models as a platform for toxicological studies regarding PFASs and their influence on neuronal subpopulations that are sensitive to estradiol. Considering the capacity that PFASs demonstrate to mimic endogenous estradiol, these cells can be used as a proxy to elucidate the impact of PFAS exposure to these particular neurons. We have shown that that extremely low doses of PFOS, PFOA, and PFHxA have divergent impacts on *kiss1* transcriptional activity on these cell types. Higher doses do not necessarily demonstrate any impact on these neurons in the context of *kiss1* transcriptional modulation. We have shown that *kiss1* transcript modulation is unique to cell type, dose, and chemical. For example, fM doses of PFOS show increased expression of *kiss1* in KTaR-1 neurons but not KTaV-3 neurons. However, fM doses of PFOA demonstrate increased *kiss1* expression in KTaV-3 neurons and a repression of *kiss1* in KTaR-1, which accurately mirrors the role of endogenous estradiol. These data illustrate the complexity and level by which these chemicals may disrupt the endocrine system at these particular neurons that are potent regulators of the HPG axis. In summary, we have created neuronal models of AVPV and arcuate neurons that recapitulate *in vivo* observations regarding estradiol sensitivity and we have demonstrated their utility in understanding the role of nuclear

estrogen receptors in mediating classical estrogen signaling as well as implicating their use as a platform for future toxicological studies regarding endocrine disrupting compounds.

References

1. L. Ahrens, W. Gerwinski, N. Theobald, R. Ebinghaus. Sources of polyfluoroalkyl compounds in the North Sea, Baltic Sea and Norwegian Sea: evidence from their spatial distribution in surface water. *Mar. Pollut. Bull.*, 60 (2010), pp. 255–260
2. N. Yamashita, K. Kannan, S. Taniyasu, Y. Horii, G. Petrick, T. Gamo. A global survey of perfluorinated acids in oceans. *Mar. Pollut. Bull.*, 51 (2005), pp. 658–668
3. C.M. Butt, U. Berger, R. Bossi, G.T. Tomy. Levels and trends of poly- and perfluorinated compounds in the arctic environment. *Sci. Total Environ.*, 408 (2010), pp. 2936–2965
4. L. Ahrens, S. Felizeter, R. Ebinghaus. Spatial distribution of polyfluoroalkyl compounds in seawater of the German bight. *Chemosphere*, 76 (2009), pp. 179–184
5. L. Ahrens, M. Plaßmann, Z. Xie, R. Ebinghaus. Determination of polyfluoroalkyl compounds in water and suspended particulate matter in the River Elbe and North Sea, Germany front. *Environ. Sci. Eng. China*, 3 (2009), pp. 152–170
6. L. Ahrens, N. Yamashita, L.W.Y. Yeung, S. Taniyasu, Y. Horii, P.K.S. Lam, R. Ebinghaus. Partitioning behavior of per- and polyfluoroalkyl compounds between pore water and sediment in two sediment cores from Tokyo Bay. *Jpn. Environ. Sci. Technol.*, 43 (2009), pp. 6969–6975
7. Y. Zushi, M. Tamada, Y. Kanai, S. Masunaga. Time trends of perfluorinated compounds from the sediment core of Tokyo Bay, Japan (1950s–2004). *Environ. Pollut.*, 158 (2010), pp. 756–763
8. M. Houde, J.W. Martin, R.J. Letcher, K.R. Solomon, D.C.G. Muir. Biological monitoring of polyfluoroalkyl substances: a review. *Environ. Sci. Technol.*, 40 (2006), pp. 3463–3473
9. S.-K. Kim, K. Kannan. Perfluorinated acids in air, rain, snow, surface runoff; and lakes: relative importance of pathways to contamination of urban lakes. *Environ. Sci. Technol.*, 41 (2007), pp. 8328–8334
10. S.-K. Kim, K. Kannan. Perfluorinated acids in air, rain, snow, surface runoff; and lakes: relative importance of pathways to contamination of urban lakes. *Environ. Sci. Technol.*, 41 (2007), pp. 8328–8334
11. M.M. Schultz, D.F. Barofsky, J.A. Field. Quantitative determination of fluorotelomer sulfonates in groundwater by LC MS/MS. *Environ. Sci. Technol.*, 38 (2004), pp. 1828–1835
12. I. Ericson, M. Nadal, B. van Bavel, G. Lindstrom, J.L. Domingo. Levels of perfluorochemicals in water samples from Catalonia, Spain: is drinking water a significant contribution to human exposure? *Environ. Sci. Pollut. Res.*, 15 (2008), pp. 614–619
13. K.J. Hansen, H.O. Johnson, J.S. Eldridge, J.L. Butenhoff, L.A. Dick. Quantitative characterization of trace levels of PFOS and PFOA in the Tennessee River. *Environ. Sci. Technol.*, 36 (2002), pp. 1681–1685
14. M.S. McLachlan, K.E. Holmstrom, M. Reth, U. Berger. Riverine Discharge of Perfluorinated Carboxylates from the European Continent. *Environ. Sci. Technol.*, 41 (2007), pp. 7260–7265

15. L. Ahrens, M. Plaßmann, Z. Xie, R. Ebinghaus. Determination of polyfluoroalkyl compounds in water and suspended particulate matter in the River Elbe and North Sea, Germany front. Environ. Sci. Eng. China, 3 (2009), pp. 152–170
16. B. Boulanger, J. Vargo, J.L. Schnoor, K.C. Hornbuckle. Detection of perfluorooctane surfactants in Great Lakes Water. Environ. Sci. Technol., 38 (2004), pp. 4064–4070
17. N. Yamashita, K. Kannan, S. Taniyasu, Y. Horii, T. Okazawa, G. Petrick, T. Gamo. Analysis of perfluorinated acids at parts-per-quadrillion levels in seawater using liquid chromatography-tandem mass spectrometry. Environ. Sci. Technol., 38 (2004), pp. 5522–5528
18. N. Yamashita, K. Kannan, S. Taniyasu, Y. Horii, G. Petrick, T. Gamo. A global survey of perfluorinated acids in oceans. Mar. Pollut. Bull., 51 (2005), pp. 658–668
19. Möller A, Ahrens L, Sturm R, Westerveld J, van der Wielen F, Ebinghaus R, de Voogt P. Distribution and sources of polyfluoroalkyl substances (PFAS) in the River Rhine watershed. Environ Pollut. 2010;158:3243–3250
20. USEPA. Perfluoroalkyl sulfonates. Proposed significant new rule. Fed. Reg., 67 (236) (2002), pp. 72854–72867
21. Karrman A, Mueller JF, van Bavel B, Harden F, Toms L-ML, Lindström G. 2006a. Levels of 12 perfluorinated chemicals in pooled Australian serum collected 2002–2003 in relation to age, gender and region. Environ Sci Technol 40:3742–3748
22. Olsen GW, Church TR, Hansen KJ, Burriss JM, Butenhoff JL, Mandel JH, et al. 2004. Quantitative evaluation of perfluorooctanesulfonate (PFOS) and other fluorochemicals in the serum of children. J Child Health 2:53–76
23. Karman A. Ericson I, van Bavel B et al. 2007. Exposure of perfluorinated chemicals through lactation: level of matched human milk and serum and a temporal trend, 1996-2004, in Sweden. Environ Health Perspect 115:226-230
24. Fields, Scott. 2007. Mapping a Course for PFCs: Transfer between Mother’s Milk and Serum. Environ Health Perspect 115(2): A97
25. Adami, H., Bergstrom, R. Mohner, M. et al. 1994. Testicular cancer in nine northern European countries. Int. J. Cancer 59:33-38
26. Moller, H. 1998. Trends in sex-ratio, testicular cancer and male reproductive hazards: are they connected? APMIS 106:232-239
27. Carlsen, E., Giwercman, A., Keiding, N. and Skakkebak, N.E. 1992. Evidence for decreasing quality of semen during past 50 years. Br. Med. J., 305:609-613
28. Andersen, A.G., Jensen, T.K., Carlsen, E. et. al. 2000. High frequency of sub-optimal semen quality in an unselected population of young men. Hum. Reprod., 15:366-372
29. Paulozzi, L.J., Erickson, J.D. and Jackson, R.J. 1997. Hypospadias rends in two US surveillance systems. Pediatrics 100: 831-834
30. Bay K, Asklund C, Skakkeback NE, Andersson AM. 2006. Testicular dysgenesis syndrome: possible role of endocrine disrupters. Best. Pract Res Clin Endocrinol Metlab 20: 77-90

31. Skakkebaek NE, Rajpert-De Meyts E, Main KM. 2001. Testicular dysgenesis syndrome: an increasingly common developmental disorder with environmental aspects. *Hum Reprod* 16: 972-978
32. Viguier-Martinez, M.C., Hochereau de Reviers, M.T., Barenton, B. and Perreau, C. 1983. Effect of a non-steroidal antiandrogen, flutamide, on the hypothalamo-pituitary axis, genital tract and testis in growing rats: endocrinological and histological data. *Acta Endocrinol.* 102: 299-306
33. Newbold, R.R. and McLachlan, J.A. 1985. Diethylstilbestrol associated defects in murine genital tract development. In McLachlan, J.A. (ed.). *Estrogen in the Environment, II: Influences on Development.* Elsevier, New York, pp. 228-313
34. Yasuda, Y., Kihara, T. and Tanimura, T. 1985. Effect of ethinyl estradiol on the differentiation of mouse fetal testis. *Teratology* 32:113-118
35. Luthra, M. and Hutson, J.M. 1989. Late-gestation exogenous oestrogen inhibits testicular descent in fetal mice despite Mullerian duct regression. *Pediatr. Surg. Int.* 4: 260-264
36. Walker, A.H., Bernstein, L., Warren, D.W. et al. 1990. The effect of in utero ethinyl oestradiol exposure on the risk of cryptorchid testis and testicular teratomas in mice. *Br. J. Cancer* 62: 599-602
37. Kelce, W.R. Lambright, C.R., Gray, L.E. Jr and Roberts, K.P. 1997. Vinclozolin and p,p'-DDE alter androgen-dependent gene expression: in vivo confirmation of an androgen receptor-mediated mechanism. *Toxicol. Appl. Pharmacol.* 142:192-200
38. Gray Jr LE, Ostby J, Furr J, Price M, Veeramachaneni DN, Parks L 2000 Perinatal exposure to the phthalates DEHP, BBP, and DINP, but not DEP, DMP, or DOTP, alters sexual differentiation of the male rat. *Toxicol Sci* 58:350-365
39. Swan SH, Main KM, Liu F, Stewart SL, Kruse RL, Calafat AM, Mao CS, Redmon JB, Ternand CL, Sullivan S, Teague JL 2005 Decrease in anogenital distance among male infants with prenatal phthalate exposure. *Environ Health Perspect* 113:1056-1061
40. McLachlan JA, Simpson E, Martin M 2006 Endocrine disrupters and female reproductive health. *Best Pract Res Clin Endocrinol Metab* 20:63-75
41. Darbre PD 2006 Environmental oestrogens, cosmetics and breast cancer. *Best Pract Res Clin Endocrinol Metab* 20:121-143
42. Fenton SE 2006 Endocrine-disrupting compounds and mammary gland development: Early exposure and later life consequences. *Endocrinology* 147:S18-S24
43. Newbold RR, Jefferson WN, Padilla-Banks E 2007 Long-term adverse effects of neonatal exposure to bisphenol A on the murine female reproductive tract. *Reprod Toxicol* 24:253-258
44. Herbst AL, Ulfelder H, Poskanzer DC 1971 Adenocarcinoma of vagina. Association of maternal stilbestrol therapy with tumor appearance in young women. *N Engl J Med* 284:878-881

45. Li S, Hursting SD, Davis BJ, McLachlan JA, Barrett JC 2003 Environmental exposure, DNA methylation and gene regulation. Lessons from diethylstilbestrol-induced cancers. *Ann NY Acad Sci* 983:161–169
46. Sheehan DM, Willingham EJ, Bergeron JM, Osborn CT, Crews D 1999 No threshold dose for estradiol-induced sex reversal of turtle embryos: how little is too much? *Environ Health Perspect* 107:155–159
47. Anway MD, Skinner MK 2006 Epigenetic transgenerational actions of endocrine disruptors. *Endocrinology* 147:S43–S49
48. Anway MD, Skinner MK 2008 Transgenerational effects of the endocrine disruptor vinclozolin on the prostate transcriptome and adult onset disease. *Prostate* 68:517–529
49. Anway MD, Cupp AS, Uzumcu M, Skinner MK 2005 Epigenetic transgenerational actions of endocrine disruptors and male fertility. *Science* 308:1466–1469
50. Christiansen S, Scholze M, Axelstad M, Boberg J, Kortenkamp A, Hass U 2008 Combined exposure to anti-androgens causes markedly increased frequencies of hypospadias in the rat. *Int J Androl* 31:241–248
51. Shono T, Suita S, Kai H, Yamaguchi Y 2004 Short-time exposure to vinclozolin in utero induces testicular maldescent associated with a spinal nucleus alteration of the genitofemoral nerve in rat. *J Pediatr Surg* 39:217–219
52. Monosson E, Kelce WR, Lambright C, Ostby J, Gray Jr LE 1999 Peripubertal exposure to the antiandrogenic fungicide, vinclozolin, delays puberty, inhibits the development of androgen-dependent tissues, and alters androgen receptor function in the male rat. *Toxicol Ind Health* 15:65–79
53. Rasier G, Parent AS, Gérard A, Lebrethon MC, Bourguignon JP 2007 Early maturation of gonadotropin-releasing hormone secretion and sexual precocity after exposure of infantile female rats to estradiol or dichlorodiphenyltrichloroethane. *Biol Reprod* 77:734–742
54. Sharif A, Baroncini M, Prevot V, Role of Glia in the Regulation of Gonadotropin-Releasing Hormone Neuronal Activity and Secretion. *Neuroendocrinology*, 2013; 98:1-15
55. Gojska M. N., Friedman Z., Belsham D. D., Direct Regulation of Gonadotropin-Releasing Hormone (GnRH) Transcription by RF-Amide-Related Peptide-3 and Kisspeptin in a Novel GnRH-Secreting Cell Line, mHypA-GnRH/GFP. *Journal of Neuroendocrinology*, 2014; 26: 888-897
56. Oakley E. A., Clifton K. D., Steiner A. R., Kisspeptin Signaling in the Brain. *Endocrine Reviews* 2009; 30(6): 713-743
57. Navarro M. V., Gottsch L. M., Chavkin C., Okamura H., Clifton K. D., Steiner A. R., Regulation of Gonadotropin-Releasing Hormone Secretion by Kisspeptin/Dynorphin/Neurokinin B Neurons in the Arcuate Nucleus of the Mouse. *The Journal of Neuroscience*, 2009; 29(38): 11869-118669
58. Seminara SB, et al. (2003) The GPR54 gene as a regulator of puberty. *N Engl J Med* 349:1614–1627

59. de Roux N, et al. (2003) Hypogonadotropic hypogonadism due to loss of function of the KiSS1-derived peptide receptor GPR54. *Proc Natl Acad Sci USA* 100:10972–10976
60. Kulin HE, Grumbach MM, Kaplan SL (1969) Changing sensitivity of the pubertal gonadal hypothalamic feedback mechanism in man. *Science* 166:1012–1013.
61. Steele RE, Weisz J (1974) Changes in sensitivity of the estradiol-LH feedback system with puberty in the female rat. *Endocrinology* 95:513–520.
62. Foster DL, Ryan KD (1979) Endocrine mechanisms governing transition into adulthood: A marked decrease in inhibitory feedback action of estradiol on tonic secretion of luteinizing hormone in the lamb during puberty. *Endocrinology* 105:896–904
63. Bronson FH (1981) The regulation of luteinizing hormone secretion by estrogen: Relationships among negative feedback, surge potential, and male stimulation in juvenile, peripubertal, and adult female mice. *Endocrinology* 108:506–516.
64. Mayer C, Acosta-Martinez M, Dubois SL, Wolfe A, Radovick S, Boehm U, Levine JE. 2010. Timing and completion of puberty in female mice depend on estrogen receptor alpha-signaling in kisspeptin neurons. *Proc Natl Acad Sci U S A* 107:22693–22698.
65. Mellon P. L., Windle J. J., Goldsmith P. C., Padula C. A., Roberts J. L., Weiner R. I., Immortalization of hypothalamic GnRH neurons by genetically targeted tumorigenesis. *Neuron* 1990; 5(1): 1-10
66. d'Anglemont de Tassigny X, Fagg LA, Dixon JP, Day K, Leitch HG, Hendrick AG, et al. Hypogonadotropic hypogonadism in mice lacking a functional Kiss1 gene. *Proc Natl Acad Sci U S A*. 2007;104(25):10714-9
67. Lapatto R, Pallais JC, Zhang D, Chan YM, Mahan A, Cerrato F, et al. Kiss1^{-/-} mice exhibit more variable hypogonadism than Gpr54^{-/-} mice. *Endocrinology*. 2007;148(10):4927-36.
68. Funes S, Hedrick JA, Vassileva G, Markowitz L, Abbondanzo S, Golovko A, et al. The KiSS-1 receptor GPR54 is essential for the development of the murine reproductive system. *Biochem Biophys Res Commun*. 2003;312(4):1357-63.
69. Irwig MS, Fraley GS, Smith JT, Acohido BV, Popa SM, Cunningham MJ, et al. Kisspeptin activation of gonadotropin releasing hormone neurons and regulation of KiSS-1 mRNA in the male rat. *Neuroendocrinology*. 2004;80(4):264-72.
70. Matsui H, Takatsu Y, Kumano S, Matsumoto H, Ohtaki T. Peripheral administration of metastin induces marked gonadotropin release and ovulation in the rat. *Biochem Biophys Res Commun*. 2004;320(2):383-8.
71. Messenger S, Chatzidaki EE, Ma D, Hendrick AG, Zahn D, Dixon J, et al. Kisspeptin directly stimulates gonadotropin-releasing hormone release via G protein-coupled receptor 54. *Proc Natl Acad Sci U S A*. 2005;102(5):1761-6. PMID: 545088
72. Navarro VM, Fernandez-Fernandez R, Castellano JM, Roa J, Mayen A, Barreiro ML, et al. Advanced vaginal opening and precocious activation of the reproductive axis by KiSS-1 peptide, the endogenous ligand of GPR54. *J Physiol*. 2004;561(Pt 2):379-86. PMID: 1665361.

73. Jayasena CN, Abbara A, Comninou AN, Nijher GM, Christopoulos G, Narayanaswamy S, et al. Kisspeptin-54 triggers egg maturation in women undergoing in vitro fertilization. *J Clin Invest.* 2014;124(8):3667-77. PMID: 4109525
74. Pineda R, Garcia-Galiano D, Roseweir A, Romero M, Sanchez-Garrido MA, Ruiz-Pino F, et al. Critical roles of kisspeptins in female puberty and preovulatory gonadotropin surges as revealed by a novel antagonist. *Endocrinology.* 2009;151(2):722-30
75. de la Iglesia HO, Blaustein JD, Bittman EL. The suprachiasmatic area in the female hamster projects to neurons containing estrogen receptors and GnRH. *Neuroreport.* 1995;6(13):1715-22.
76. de la Iglesia HO, Meyer J, Schwartz WJ. Lateralization of circadian pacemaker output: Activation of left- and right-sided luteinizing hormone-releasing hormone neurons involves a neural rather than a humoral pathway. *J Neurosci.* 2003;23(19):7412-4
77. Abizaid A, Horvath B, Keefe DL, Leranth C, Horvath TL. Direct visual and circadian pathways target neuroendocrine cells in primates. *Eur J Neurosci.* 2004;20(10):2767-76
78. Chappell PE, White RS, Mellon PL. Circadian gene expression regulates pulsatile gonadotropin-releasing hormone (GnRH) secretory patterns in the hypothalamic GnRH-secreting GT1-7 cell line. *J Neurosci.* 2003;23(35):11202-13
79. Hickok JR, Tischkau SA. In vivo circadian rhythms in gonadotropin-releasing hormone neurons. *Neuroendocrinology.* 2009;91(1):110-20
80. Tonsfeldt KJ, Goodall CP, Latham KL, Chappell PE. Oestrogen induces rhythmic expression of the Kisspeptin-1 receptor GPR54 in hypothalamic gonadotrophin-releasing hormone-secreting GT1-7 cells. *J Neuroendocrinol.* 2011;23(9):823-30. PMID: 3243730.
81. erbison AE. Estrogen positive feedback to gonadotropin-releasing hormone (GnRH) neurons in the rodent: the case for the rostral periventricular area of the third ventricle (RP3V). *Brain Res Rev.* 2008;57(2):277-87.
82. Kauffman AS, Clifton DK, Steiner RA. Emerging ideas about kisspeptin- GPR54 signaling in the neuroendocrine regulation of reproduction. *Trends Neurosci.* 2007;30(10):504-11
83. Robertson JL, Clifton DK, de la Iglesia HO, Steiner RA, Kauffman AS. Circadian regulation of Kiss1 neurons: implications for timing the preovulatory gonadotropin-releasing hormone/luteinizing hormone surge. *Endocrinology.* 2009;150(8):3664-71. PMID: 2717859.
84. Van der Beek EM, Horvath TL, Wiegant VM, Van den Hurk R, Buijs RM. Evidence for a direct neuronal pathway from the suprachiasmatic nucleus to the gonadotropin-releasing hormone system: combined tracing and light and electron microscopic immunocytochemical studies. *J Comp Neurol.* 1997;384(4):569-79.
85. Kinoshita M, Tsukamura H, Adachi S, Matsui H, Uenoyama Y, Iwata K, et al. Involvement of central metastin in the regulation of preovulatory luteinizing hormone surge and estrous cyclicity in female rats. *Endocrinology.* 2005;146(10):4431-6.
86. Wakabayashi Y, Nakada T, Murata K, Ohkura S, Mogi K, Navarro VM, et al. Neurokinin B and dynorphin A in kisspeptin neurons of the arcuate nucleus participate in generation

- of periodic oscillation of neural activity driving pulsatile gonadotropin-releasing hormone secretion in the goat. *J Neurosci.* 2010;30(8):3124-32.
87. Hu MH, Li XF, McCausland B, Li SY, Gresham R, Kinsey-Jones JS, et al. Relative Importance of the Arcuate and Anteroventral Periventricular Kisspeptin Neurons in Control of Puberty and Reproductive Function in Female Rats. *Endocrinology.* 2015;156(7):2619-31. PMID: 4475719
 88. Belsham DD, Cai F, Cui H, Smukler SR, Salapatek AM, Shkreta L. Generation of a phenotypic array of hypothalamic neuronal cell models to study complex neuroendocrine disorders. *Endocrinology.* 2004;145(1):393-400
 89. Gingerich S, Wang X, Lee PK, Dhillon SS, Chalmers JA, Koletar MM, et al. The generation of an array of clonal, immortalized cell models from the rat hypothalamus: analysis of melatonin effects on kisspeptin and gonadotropin-inhibitory hormone neurons. *Neuroscience.* 2009;162(4):1134-40.
 90. Mittelman-Smith MA, Wong AM, Kathiresan AS, Micevych PE. Classical and membrane-initiated estrogen signaling in an in vitro model of anterior hypothalamic kisspeptin neurons. *Endocrinology.* 2015;156(6):2162-73. PMID: 4430613
 91. Treen AK, Luo V, Chalmers JA, Dalvi PS, Tran D, Ye W, et al. Divergent Regulation of ER and Kiss Genes by 17beta-Estradiol in Hypothalamic ARC Versus AVPV Models. *Mol Endocrinol.* 2016;30(2):217-33
 92. Kriegsfeld LJ, Silver R, Gore AC, Crews D. Vasoactive intestinal polypeptide contacts on gonadotropin-releasing hormone neurones increase following puberty in female rats. *J Neuroendocrinol.* 2002;14(9):685-90
 93. Gerhold LM, Wise PM. Vasoactive intestinal polypeptide regulates dynamic changes in astrocyte morphometry: impact on gonadotropin-releasing hormone neurons. *Endocrinology.* 2006;147(5):2197-202
 94. Miller BH, Olson SL, Levine JE, Turek FW, Horton TH, Takahashi JS. Vasopressin regulation of the proestrous luteinizing hormone surge in wild-type and Clock mutant mice. *Biol Reprod.* 2006;75(5):778-84
 95. Vida B, Deli L, Hrabovszky E, Kalamatianos T, Caraty A, Coen CW, et al. Evidence for suprachiasmatic vasopressin neurones innervating kisspeptin neurones in the rostral periventricular area of the mouse brain: regulation by oestrogen. *J Neuroendocrinol.* 2010;22(9):1032-9
 96. Piet R, Fraissenon A, Boehm U, Herbison AE. Estrogen permits vasopressin signaling in preoptic kisspeptin neurons in the female mouse. *J Neurosci.* 2015;35(17):6881-92.
 97. Rapisarda JJ, Bergman KS, Steiner RA, Foster DL (1983) Response to estradiol inhibition of tonic luteinizing hormone secretion decreases during the final stage of puberty in the rhesus monkey. *Endocrinology* 112:1172–1179
 98. Monroe DG, Johnsen SA, Subramaniam M, et al. Mutual antagonism of estrogen receptors alpha and beta and their preferred interactions with steroid receptor coactivators in human osteoblastic cell lines. *J Endocrinol.* 2003;176:349–57.

99. Li, D., Mitchell, D., Luo, J. et al. (2007) Estrogen regulates KiSS1 gene expression through estrogen receptor alpha and SP protein complexes. *Endocrinology*, 148, 4821–4828
100. Lindstrom AB, Strynar MJ and Libelo EL. Polyfluorinated compounds: past, present, and future. *Environ Sci Technol* 2011; 45: 7954–7961
101. Grandjean P. Clapp R. Perfluorinated Alkyl Substances: Emerging Insights Into Health Risks. *New Solut* 2015; 2: 147-63
102. Diamanti- Kandarakis E, Bourguignon JP, Giudice LC, Hauser R, Prins GS, Soto AM, Zoeller RT and Gore AC (2009) Endocrine- disrupting chemicals: an Endocrine Society scientific statement. *Endocr Rev* 30, 293–342.
103. CSID:67068, <http://www.chemspider.com/Chemical-Structure.67068.html> (accessed 20:20, Oct 3, 2016)
104. CSID:9180, <http://www.chemspider.com/Chemical-Structure.9180.html> (accessed 20:21, Oct 3, 2016)
105. CSID:60864, <http://www.chemspider.com/Chemical-Structure.60864.html> (accessed 20:21, Oct 3, 2016)
106. Skorupskaite K, George JT, Anderson RA. The kisspeptin-GnRH pathway in human reproductive health and disease. *Human Reproduction Update*. 2014;20(4):485-500. doi:10.1093/humupd/dmu009.